nks
Nordisk kernesikkerhedsforskning
Norrænar kjarnöryggisrannsóknir
Pohjoismainen ydinturvallisuustutkimus
Nordisk kjernesikkerhetsforskning
Nordisk kärnsäkerhetsforskning
Nordic nuclear safety research

NKS-130
ISBN 87-7893-192-4

Wire System Aging Assessment and Condition Monitoring (WASCO)

Paolo F. Fantoni
Institutt for energiteknikk, Norway

Anders Nordlund
Chalmers University of Technology, Sweden

April 2006

Abstract

Nuclear facilities rely on electrical wire systems to perform a variety of functions for successful operation. Many of these functions directly support the safe operation of the facility; therefore, the continued reliability of wire systems, even as they age, is critical. Condition Monitoring (CM) of installed wire systems is an important part of any aging program, both during the first 40 years of the qualified life and even more in anticipation of the license renewal for a nuclear power plant. This report describes a method for wire system condition monitoring, developed at the Halden Reactor Project, which is based on Frequency Domain Reflectometry. This method resulted in the development of a system called LIRA (LIne Resonance Analysis), which can be used on-line to detect any local or global changes in the cable electrical parameters as a consequence of insulation faults or degradation. LIRA is composed of a signal generator, a signal analyser and a simulator that can be used to simulate several failure/degradation scenarios and assess the accuracy and sensitivity of the LIRA system. Chapter 5 of this report describes an complementary approach based on positron measurement techniques, used widely in defect physics due to the high sensitivity to micro defects, in particular open volume defects. This report describes in details these methodologies, the results of field experiments and the proposed future work.

Key words

Condition monitoring, cable aging, transmission lines, hot spot detection, fault detection, frequency domain reflectometry, time domain reflectometry, standing wave reflectometry, LIRA, positron

NKS-130
ISBN 87-7893-192-4

Electronic report, April 2006

The report can be obtained from
NKS Secretariat
NKS-775
P.O. Box 49
DK - 4000 Roskilde, Denmark

Phone +45 4677 4045
Fax +45 4677 4046
www.nks.org
e-mail nks@nks.org

Wire System Aging Assessment and Condition Monitoring (WASCO)

Paolo F. Fantoni, IFE, Norway
Anders Nordlund, Chalmers University of Technology, Sweden

Keywords

Condition monitoring, cable aging, transmission lines, hot spot detection, fault detection, frequency domain reflectometry, time domain reflectometry, standing wave reflectometry, LIRA, positron

Abstract

Nuclear facilities rely on electrical wire systems to perform a variety of functions for successful operation. Many of these functions directly support the safe operation of the facility; therefore, the continued reliability of wire systems, even as they age, is critical. Condition Monitoring (CM) of installed wire systems is an important part of any aging program, both during the first 40 years of the qualified life and even more in anticipation of the license renewal for a nuclear power plant. This report describes a method for wire system condition monitoring, developed at the Halden Reactor Project, which is based on Frequency Domain Reflectometry. This method resulted in the development of a system called LIRA (LIne Resonance Analysis), which can be used on-line to detect any local or global changes in the cable electrical parameters as a consequence of insulation faults or degradation. LIRA is composed of a signal generator, a signal analyser and a simulator that can be used to simulate several failure/degradation scenarios and assess the accuracy and sensitivity of the LIRA system. Chapter 5 of this report describes an complementary approach based on positron measurement techniques, used widely in defect physics due to the high sensitivity to micro defects, in particular open volume defects. This report describes in details these methodologies and the results of performed field experiments. The work has been carried on with the support from the Nordic Nuclear Safety Research (NKS), in the framework of the NKS-R Program 2005 (WASCO).

TABLE OF CONTENTS

1. INTRODUCTION

There is a continued interest worldwide in the safety aspects of electrical wire (cable) system aging in industrial installations, including operating nuclear power plants. Aging of a wire system can result in loss of critical functions of the equipment energized by the system, or in loss of critical information relevant to the decision making process and operator actions. In either situation, unanticipated or premature aging of a wire system can lead to unavailability of equipment important to safety and compromise public health and safety. An additional issue is related to the life extension of existing plants, beyond the normal life of 40 years. Under these conditions, it is important to assess the degradation of safety related electric cables and their expected residual lifetime, both in normal operation and during/after design base accidents (DBA).

The U.S. White House National Science and Technology Council Committee on Technology has issued a report in 2000 [1] where safety issues on wire systems were addressed. The conclusions of this report are important to understand the weak points of the current status and which topics should be addressed in future research. The recommendations of the Committee can be summarised as follows:

- Increase co-operation between industry and research institutes, also internationally.
- Improve design and functionality of wire systems.
- Develop advanced wire system condition monitoring techniques.

To the same conclusion arrived research efforts from the IAEA [2] and the OECD NEA [3].

Current techniques to evaluate aging properties of electric cables include mechanical and electric properties tests [2,3]. While known to be difficult, advancements in detection systems and computerised data analysis techniques may allow ultimate use of electrical testing to predict future behaviour and residual life of cables, also in DBA conditions.

While a significant amount of research has been performed related to wire system aging and safety, there are still a number of issues that remain unresolved and should be addressed and a survey to identify the current state and results of the research in the field was prepared by the Halden Project [4].

As a result of this preliminary study, the Halden Project is now developing a method based on transmission line theory with the aim to develop a tool to be used on-site and capable to detect and locate cable defects and aging conditions. This method is called LIRA (Line Resonance Analysis) and preliminary results are already available.

Chapter 3 of this report describes the theory on which LIRA is based, while chapter 4 shows some test performed to qualify the three modules that all together make LIRA a complete condition monitoring system. Chapter 5 describes how LIRA should be used to assess the actual condition of a monitored wire system and chapter 6 gives some ideas of the future work that is still needed.

2. CONDITION MONITORING TECHNIQUES BASED ON CABLE ELECTRICAL PARAMETERS

Beside LIRA, other emerging techniques exist, where the cable electrical parameters are taken as condition indicators: among these techniques, the *Broadband Impedance Spectroscopy* (BIS) from Boeing (USA) [5] and the *Dielectric Loss Measurement* from EDF, France [6].

The BIS method has been originally studied by Boeing and it is now a topic of research in a co-operation among Boeing, Brookhaven National Lab. and the NRC, in USA. This method, as LIRA, is based on transmission line theory like LIRA, but with many differences in the approach. In particular, the hot spot detection is based on comparison between the actual behavior of the input impedance and the expected simulated behavior.

EDF, France, is working with a very low frequency method trying to estimate the insulation dissipation factor (also known as *tanδ*) that, in the frequency order of 10^{-1} - 10^{-4} Hz, is sensitive to the material degradation. This method could be applied to evaluate the global state of a wiring system.

Other contributions to Frequency Domain Reflectometry techniques can be found in the co-operative work of the Yonsei University of Seoul, Korea, and the University of South Carolina [7,8], where they are studying a method based on Joint Time-Frequency Domain Reflectometry (JTFDR). Other contributions can be found in Taiwan [9] and at the University of Utah, USA [10].

3. THE LIRA METHOD

3.1 Transmission Line Theory

A transmission line [12,13] is the part of an electrical circuit providing a link between a generator and a load. The behavior of a transmission line depends by its length in comparison with the **wavelength** λ of the electric signal traveling into it. The wavelength is defined as:

$$\lambda = v/f \tag{1}$$

where v is the speed of the electric signal in the wire and f the frequency of the AC signal.

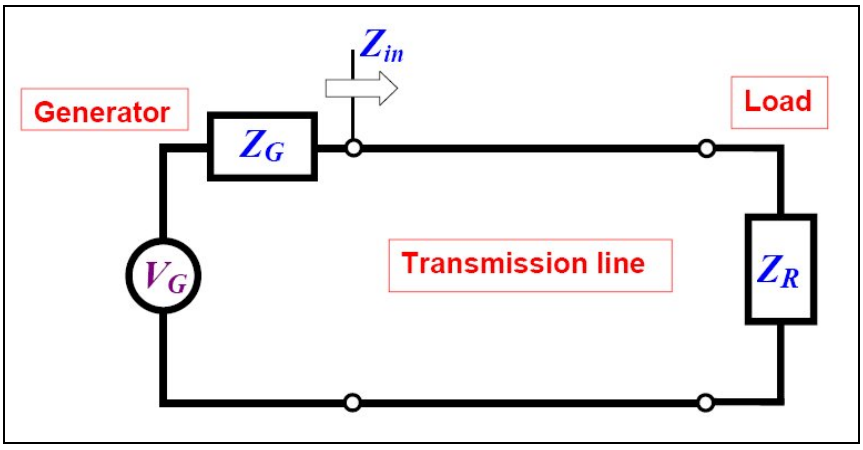

Figure 1. Transmission line components

When the transmission line length is much lower than the wavelength, as it happens when the cable is short and the signal frequency is low, the line has no influence on the circuit behavior and the circuit impedance (Z_{in}), as seen from the generator side, is equal to the load impedance at any time.

However, if the line length and/or the signal frequency are high enough, so that $L \geq \lambda$, the line characteristics take an important role and the circuit impedance seen from the generator does not match the load, except for some very particular cases.

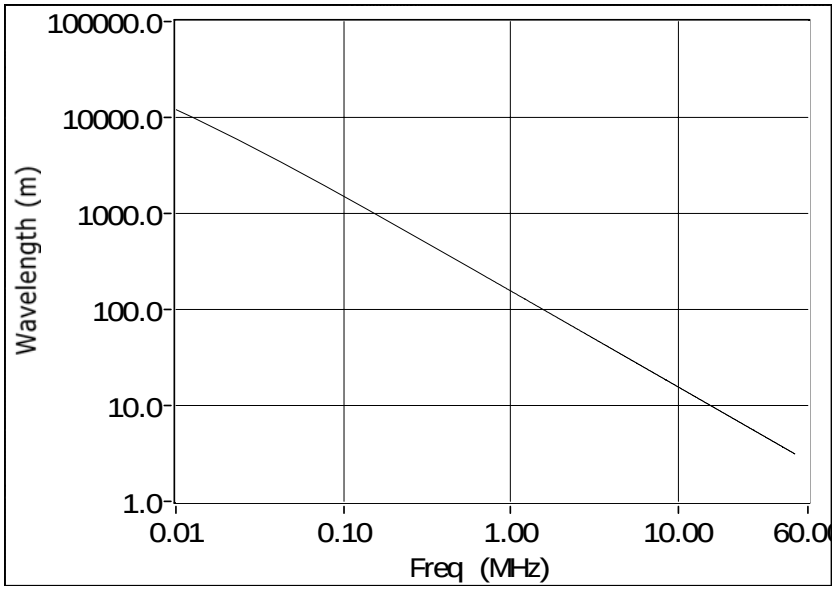

Figure 2. Relation between frequency and wavelength

To give an idea of applicable frequencies for transmission line applications, Figure 2 shows the critical wire lengths (when L=λ) as a function of the applied frequency, for a typical power cable.

To study the behaviour of a transmission line at high frequencies, it is convenient to represent it with its equivalent lumped parameters, as depicted in *Figure 3*.

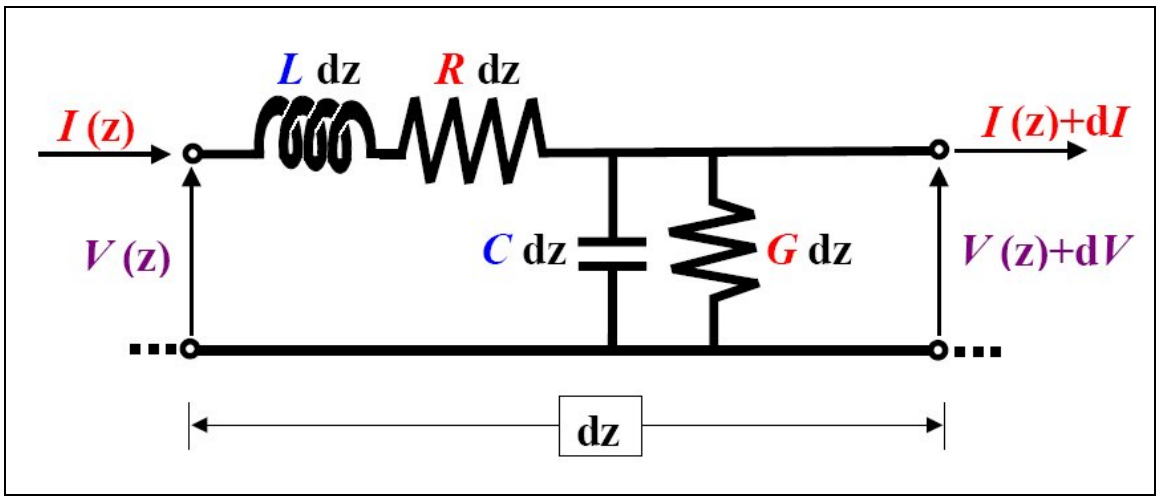

Figure 3. Transmission line equivalent circuit

Here L represents the conductor inductance for unit length (H/m), R the conductor resistance for unit length (Ω/m), G the insulation conductance (S/m) and C the insulation capacitance (F/m). If we write the equations for this electric circuit, we arrive to the two following relations:

$$(V + dV) - V = -(Rdz + j\omega Ldz)I \tag{2}$$

$$dI = -(Gdz + j\omega Cdz)(V + dV) \tag{3}$$

that results in the so called **telegraphers equations**:

$$\frac{dV}{dz} = -(R + j\omega L)I \tag{4}$$

$$\frac{dI}{dz} = -(G + j\omega C)V \tag{5}$$

These equations can be solved by differentiating with respect to z and including eq. (2) and (3), arriving at the so called **telephonists equations**:

$$\frac{d^2V}{dz^2} = (R + j\omega L)(G + j\omega C)V \tag{6}$$

$$\frac{d^2I}{dz^2} = (R + j\omega L)(G + j\omega C)I \tag{7}$$

The solution of the differential equations (6) and (7) bring to the two following equations, describing the behaviour of V and I along the wire:

$$V(z) = V^+e^{-\gamma z} + V^-e^{\gamma z} \tag{8}$$

$$I(z) = {}^{1}\!/_{Z_0}\left(V^+e^{-\gamma z} - V^-e^{\gamma z}\right) \tag{9}$$

Where V^+ and V^- are the forward and reflected wave voltage.

Although equations (8) and (9) need some boundary conditions (at the generator and load side) to solve the constants V^+ and V^-, it is possible to derive some interesting observations from them:

- Both the voltage V and the current I are composed of 2 components, where the first is a wave travelling towards the load (the incident wave) and the second is a wave travelling back towards the generator (the reflected wave).
- Two important parameters are visible in these equations, the two parameters that affect the overall behaviour of a transmission line. They are:
    - **The propagation constant γ:** it can be expanded to:

$$\gamma = \sqrt{(R + j\omega L)(G + j\omega C)} \tag{10}$$

      γ is then a complex value depending by the 4 electrical parameters R,L,G and C and the signal frequency. It can be written as **γ = α + jβ**, where α is known as the **attenuation constant** and β the **phase constant.** The reason for this terminology becomes apparent if we write equation (8) expanding γ:

$$V(z) = V^+e^{-\alpha z}e^{-j\beta z} + V^-e^{\alpha z}e^{j\beta z} \tag{11}$$

      Here the two phasor components representing the two waves have a magnitude affected by α and a phase affected by β.

    - **The characteristic impedance Z_0:** it can be expanded to:

$$Z_0 = \sqrt{\frac{R + j\omega L}{G + j\omega C}} \tag{12}$$

It is a complex parameter that can be considered as the impedance seen by the incident wave or reflected wave separately. The total cable impedance (which includes the incident and reflected waves) has nothing to do with this number. Note also that the characteristic impedance does not depend by the cable length.

Both γ and Z_0 have a strong dependence by the signal frequency. In the high frequency range, above 1 MHz, $\omega L >> R$ and $\omega C >> G$, so that the following relations apply to these important parameters:

$$Z_0 = \sqrt{\frac{L}{C}} \tag{13}$$

$$\beta = \omega\sqrt{LC} \tag{14}$$

which show that Z_0 becomes real at high frequency and independent from signal frequency. The real part (α) of the propagation constant, at high frequency, flattens to:

$$\alpha = \frac{R}{2}\sqrt{\frac{C}{L}} \tag{15}$$

that is proportional to the wire resistance. Equation (15) could lead to the wrong impression that the wire losses reach a maximum at high frequencies, depending by the values of R, C and L. Unfortunately, R itself is not a constant but, because of the skin effect, it increases with the square root of frequency. The overall effect, assuming C and L constant with frequency (L decreases slightly with f) is that the wire attenuation increases with the square root of *f* and linearly with the cable length (α is usually expressed in dB/km), setting a limit to the maximum frequency and wire length to efficiently transmit a signal along a cable without amplification.

The phase constant is related to the signal wavelength by the following relation:

$$\beta = \frac{2\pi}{\lambda} = \frac{\omega}{v} \tag{16}$$

where ω is the signal radial frequency and v is the *phase velocity* of the electromagnetic field in the cable dielectric, which at high frequencies flattens to:

$$v = \frac{1}{\sqrt{LC}} \tag{17}$$

Equation (1) and (17) state an important property of transmission lines, which can be formulated as follows: “The wavelength of a high frequency signal in a wire is inversely proportional to the square root of the product LC”. In other words, changes in L and C such that their product remains constant do not cause any change in the signal wavelength and β. This is one of the main concerns about the use of transmission line techniques for cable diagnostics and it will be addressed later in this report.

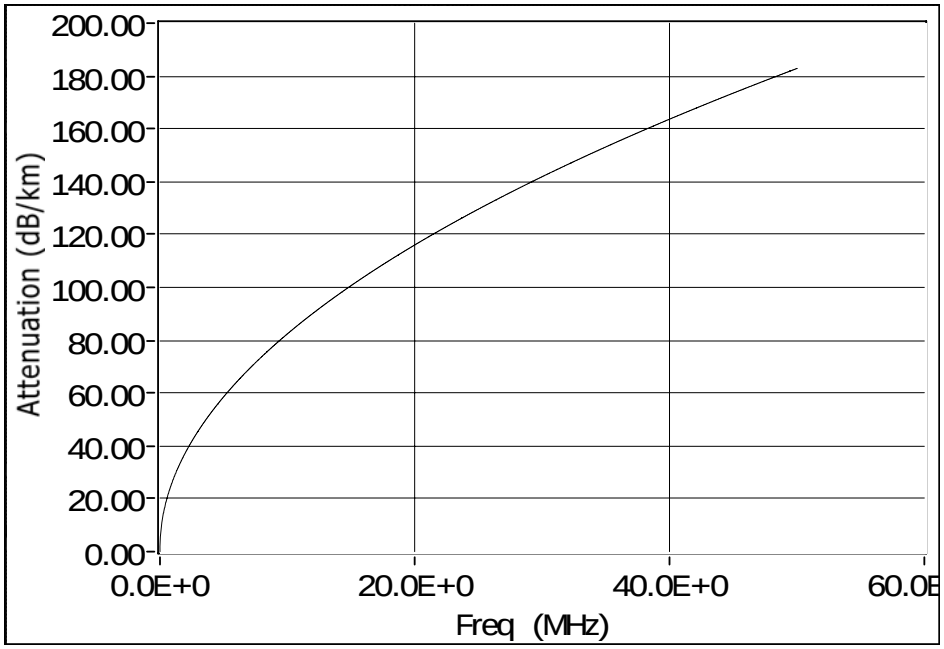

Figure 4. Cable attenuation vs. frequency

Figure 4 shows the relation of wire attenuation with frequency, for a typical cable.

3.1.1 Solution of the wave equations

Equations (8) and (9) can be solved using two boundary conditions for the calculation of V^+ and V^- (V^+ and V^- are the magnitude of the incident and reflected wave, respectively). In transmission line theory, it is often used a direction axis with the origin at the load, which increases towards the generator. The application of this transformation to eqs. (8) and (9) brings to:

$$V(d) = V^+ e^{\gamma d} + V^- e^{-\gamma d} \tag{18}$$

$$I(d) = {}^{1}\!/_{Z_0} \left(V^+ e^{\gamma d} - V^- e^{-\gamma d} \right) \tag{19}$$

At the load (d=0) we can write:

$$V(0) = V^+ + V^- \tag{20}$$

$$I(0) = \frac{1}{Z_0}\left(V^+ - V^- \right) \tag{21}$$

If we call Z_L the load impedance, since $V(0)/I(0) = Z_L$, substituting in eqs. (20) and (21):

$$\frac{V^-}{V^+} = \Gamma_L = \frac{Z_L - Z_0}{Z_L + Z_0} \tag{22}$$

Where Γ_L is the *load reflection coefficient*. Using this new parameter in eqs. (18) and (19) we arrive to:

$$V(d) = V^+ e^{\gamma d}\left(1 + \Gamma_L e^{-2\gamma d} \right) \tag{23}$$

$$I(d) = \frac{V^+ e^{\gamma d}}{Z_0}\left(1 - \Gamma_L e^{-2\gamma d}\right) \tag{24}$$

Γ_L is the ratio of the reflected wave magnitude (V^-) to the incident wave magnitude (V^+) and represents the extent of the reflection at the load. The load reflection coefficient is 0 when the line is matched, that is when the load impedance Z_L matches the characteristic impedance Z_0. At the two extremes, it is -1 when the load is shorted and +1 when the termination is open ($Z_L = \infty$). It is here convenient to define a *generalized reflection coefficient* Γ_d:

$$\Gamma_d = \Gamma_L e^{-2\gamma d} \tag{25}$$

so that eqs. (23) and (24) become:

$$V(d) = V^+ e^{\gamma d}\left(1 + \Gamma_d\right) \tag{26}$$

$$I(d) = \frac{V^+ e^{\gamma d}}{Z_0}\left(1 - \Gamma_d\right) \tag{27}$$

Eqs. (26) and (27) define the distribution of voltage and current along the wire as a function of the characteristic impedance and the generalized reflection coefficient. Note that, although the load reflection coefficient can be real, the generalized reflection coefficient is always complex.

3.1.2 The Line Impedance

It is now possible to define a *Line Impedance* Z_d, which is the most important variable in the LIRA system:

$$Z_d = \frac{V(d)}{I(d)} = Z_0 \frac{1 + \Gamma_d}{1 - \Gamma_d} \tag{28}$$

For $d=L$, the line impedance is the value Z_{in} seen from the generator, so that the all circuit is equivalent to the one shown in Figure 5.

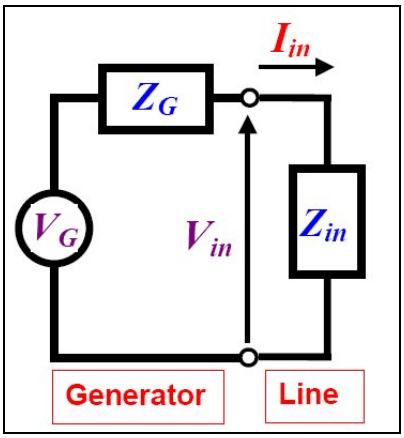

Figure 5. Line impedance as a substitution of the transmission line

To study the distribution of Z_d along the wire, remind the definition of Γ_d from eq. (25), that can be rewritten as:

$$\Gamma_d = \Gamma_L e^{-2\alpha d} e^{-2j\beta d} \tag{29}$$

which is a pseudo-periodic function of d (it is periodic in a loss-less cable, when α = 0). If the load reflection coefficient Γ_L is real and positive (load higher than the characteristic impedance), function (28) has its maximum values for:

$$2\beta d = 2 \times \frac{2\pi}{\lambda} d = 2\pi k, \quad with \quad k = 0...n \tag{30}$$

That is:

$$d = \frac{\lambda}{2} k \quad , k = 0...n \tag{31}$$

Using the same procedure, line impedance minimum values are found at:

$$d = \frac{\lambda}{4}(2k+1) \quad , k = 0...n \tag{32}$$

The magnitude of the maximum and minimum impedance values depend by the load reflection coefficient and the attenuation α. The phase of the line impedance, corresponding to the maximum and minimum magnitude, is zero, so that the impedance becomes real and this condition is called a resonance point. This is the main concept at the base of the LIRA system. Resonance points (also called phase zero-crossing) do not depend by the cable losses, which is difficult to estimate, but only by the wire wavelength and at the very last by the parameters affecting the wavelength. As shown in eqs. (1) and (17), these parameters are the signal frequency (user controlled) and the insulation parameters L and C. At a sufficiently high frequency, when R and G do not affect the impedance behaviour, monitoring the shift of the line input impedance phase from a resonance condition, has the significant effect of monitoring any small change in the two electrical parameters that characterize the cable insulation. In other words:

Line input impedance phase shift from resonance is an effective ***condition indicator*** *for the wire insulation.*

A point to be made at this time is that the line impedance, as defined in eq. (28), is a function of d, the distance from the load on the cable. If one should go along a cable taking impedance measurements, this method would be completely unfeasible for our purpose. The good news is that, considering the inverse relationship between wavelengths and frequencies, estimating impedances along the wire is perfectly equivalent to estimating it at **one single position** and changing the signal frequency. The selected position is the beginning of the cable, generator side, at *d=L*. *Figure 6* shows a real example of line impedance as a function of frequency (it is a 10m RG-58 coaxial cable). The decreasing peaks in the amplitude are a consequence of the line attenuation.

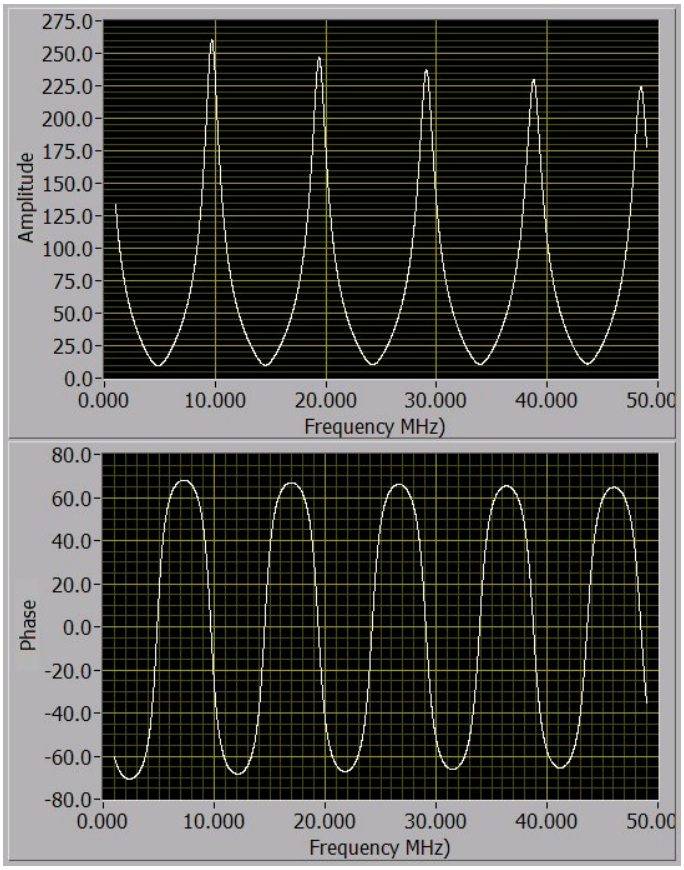

Figure 6. Line Input Impedance, amplitude and phase, as a function of signal frequency (picture taken from LIRA Simulator)

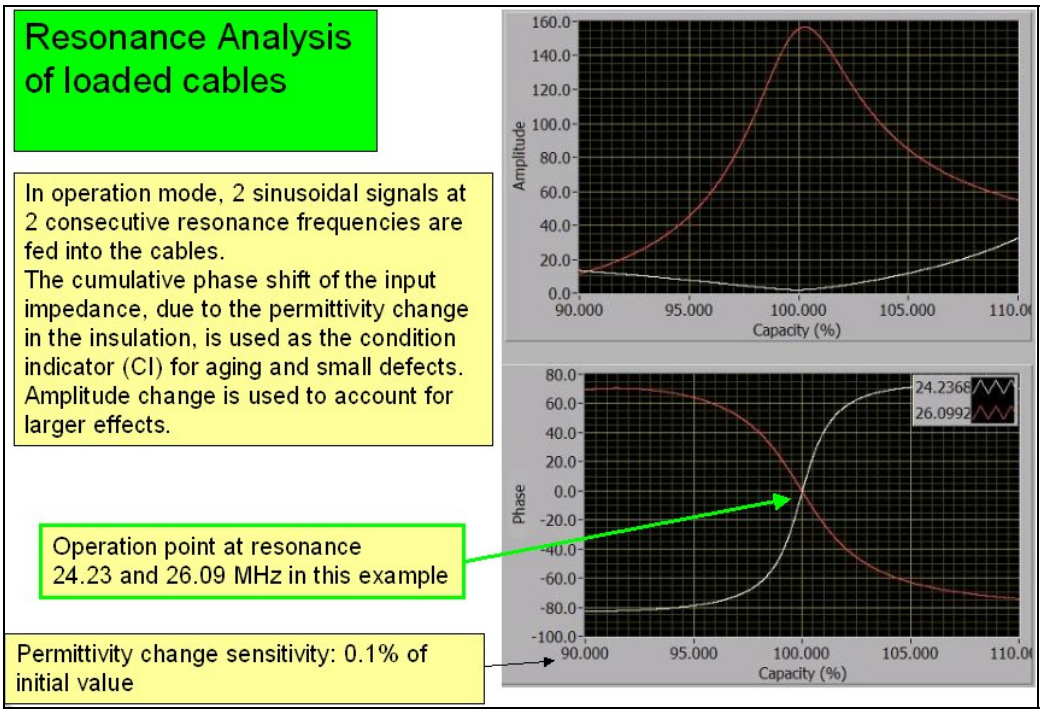

Figure 7. Sensitivity of line impedance phase to wire capacitance change

Figure 7 shows the sensitivity of the line impedance phase to changes of the wire capacitance (related to the insulation permittivity, or complex dielectric function). In this example the effect on two consecutive resonance frequencies are shown. Resonance frequencies are strongly dependent by the cable length and the values of L and C.

3.1.3 Effects of loading on the line impedance phase

Degradation or failure at the equipment attached to the cable end produce effects qualitatively similar to those produced by the global cable degradation (as seen in the previous chapter, local faults are not affected). It is important then to detect and discriminate loading effects from cable characteristic changes.

The load is characterized by a combination of resistance, inductor and capacitance, as depicted in Figure 8.

The total load impedance is equivalent to:

$$Z_L = \left(R + j\omega L\right) \,\|\, {}^{1}\!\!\diagup\!\!{}_{j\omega C}$$

Where the $\|$ symbol refers to the parallel operator.

The effect of L and C is to introduce an imaginary component into the *reflective coefficient* Γ, which causes a phase shift in the input impedance equivalent to that caused by changes in the distributed capacitance. R does not produce any effect in the phase component, but only in the amplitude value, and L does not suffer significant changes after degradation or incipient failures and, however, its effects are similar to those produced by changes in C. The following discussion is then limited to the effects produced by the load capacitance C.

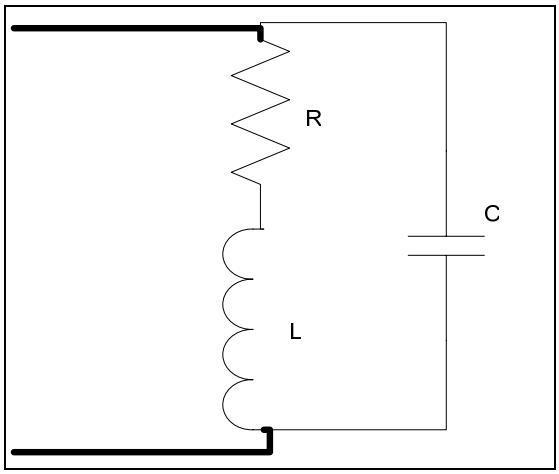

Figure 8. Load equivalent circuit

Figure 9 to Figure 11 show the cable input impedance phase as a function of C_d change and clearly show the problem and its dimension. Figure 9 shows the operating point for a 500m, 50Ω Z_0 cable with open end, at 2 resonance frequencies of 692kHz and 791kHz. The reference distributed cable capacity is C_d=101pF/m (coaxial RG58 cable). The sensitivity to C_d is 10deg/% for each frequency component that means 10deg/pF/m for component. Figure 10 and Figure 11 shows the effect of adding a shunt capacity of 100pF and 1000pF at the load, respectively.

From these pictures it is easy to see that adding 1000pF at the load has the same effect of **increasing** C_d by 4% (4pF/m). These considerations lead to the following conclusions:

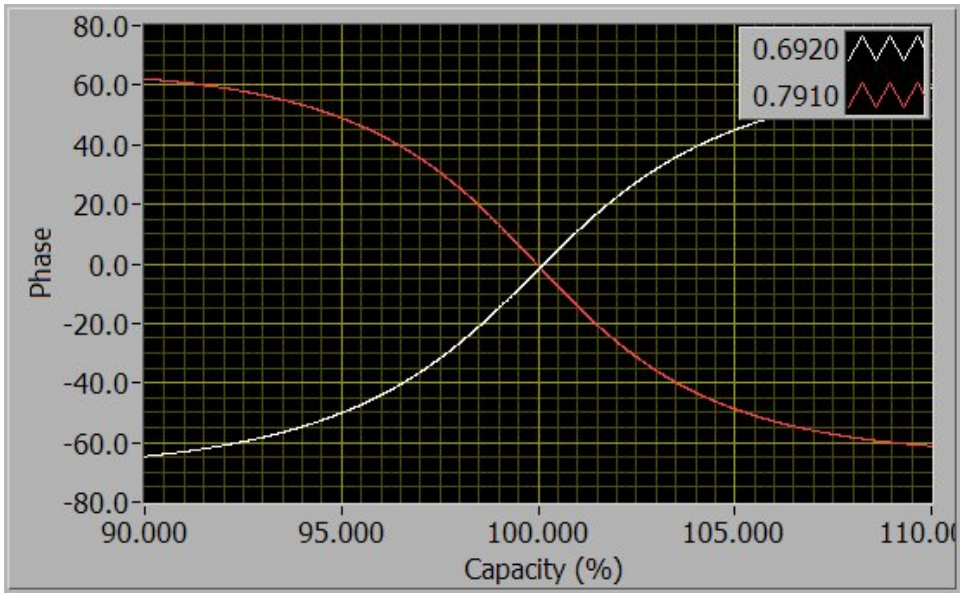

Figure 9. 500m wire, 692-791kHz, resistive load

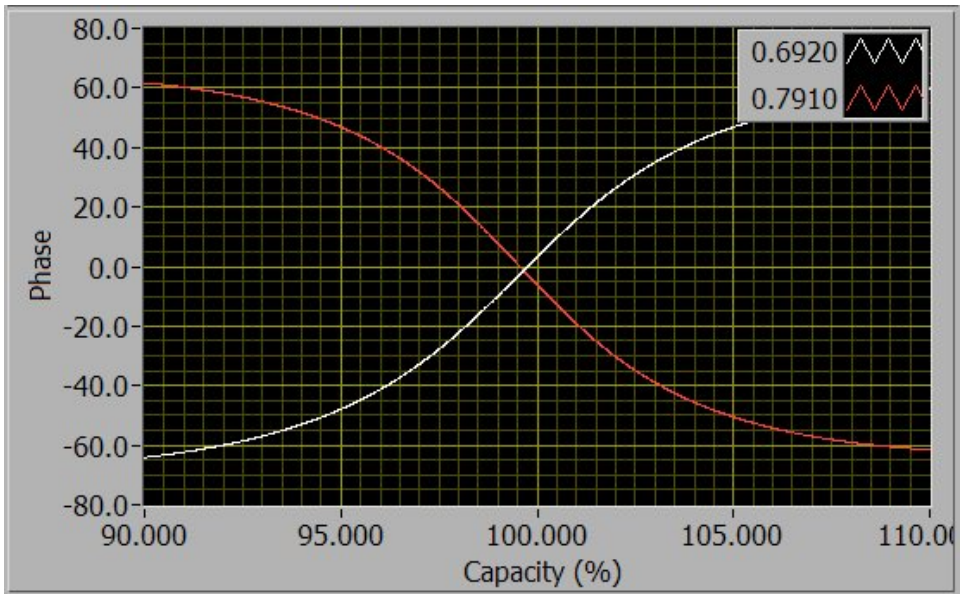

Figure 10. 500m wire, 692-791kHz, 100pF load

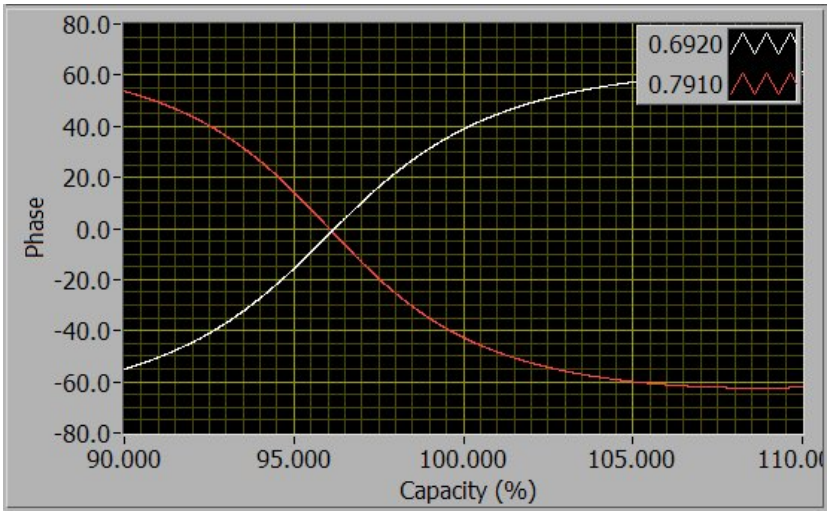

Figure 11. 500m wire, 692-791kHz, 1000pF load

- Small shunt capacity changes at the load (< 50pF) have only negligible effects on the impedance phase.
- The two effects add up producing an overall phase shift that can be caused by the wire, the load or both.
- The above results correspond to a 500m cable at 700 kHz. Capacitative loading effects have a strong sensitivity to the operating frequency. Higher frequencies result in higher phase shifts for the same load capacitance change. To give an example, a 50 km cable operating at 4 kHz, a 10000 pF change at the load produces only 4 deg shift in the impedance phase, the same effect that a 0.8% change in the distributed cable capacity would get. This point is clearly shown in Figure 12, where the equivalent C_d is plotted against the load change, for different cable lengths (remember that the operating frequency is inversely proportional to cable length).

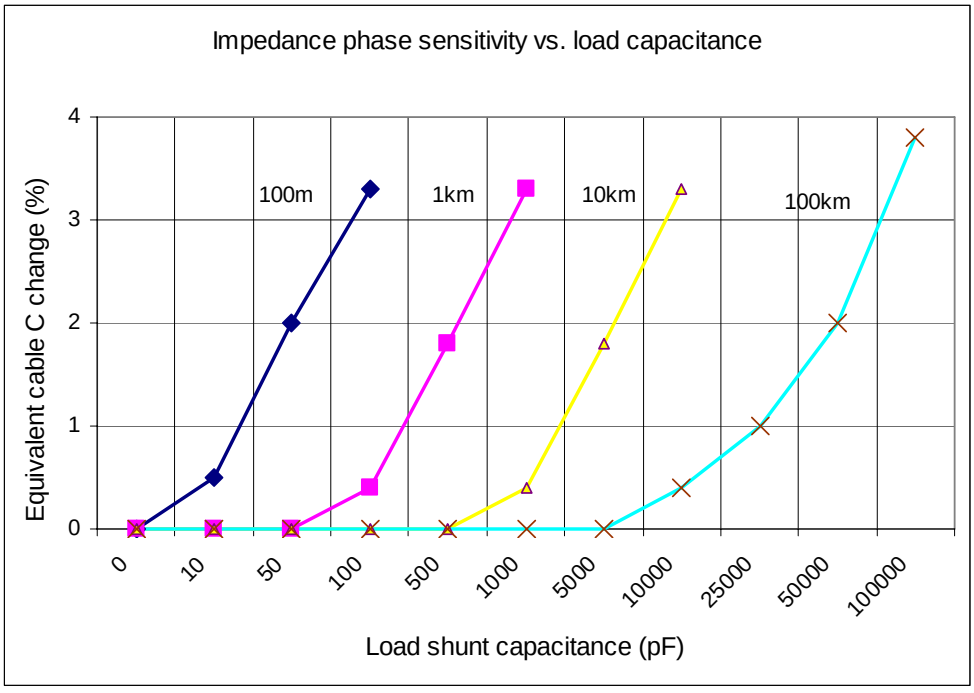

Figure 12. Sensitivity to load capacitance changes

The second point suggests having a method to estimate the load shunt capacity and detect any change of it due to degradation and/or failure.

LIRA can estimate on-line the shunt capacity at the load using a technique called Resonance Frequency Spread (RFS), developed at the HRP.

3.1.3.1 Resonance Frequency Spread

The resonance frequencies change slightly when the cable capacitance or the load capacitance change. However, when the change is in the cable (both global and local), the ratio between a resonance frequency before and after the capacity change is constant through the spectrum, that is it is the same for any resonance frequency. The upper graph in Figure 13 shows this ratio before any change (which is obviously 1.0 at any frequency), while the middle graph shows the consequence of a cable change (simulated test). In this case the ratio of any resonance frequency is 1.02 at any resonance point. However, when a load capacitance change is sensed, the resulting graph is like the bottom one in Figure 13, where a trend toward lower ratios is evident. This example simulates a 500m cable with a 2 pF/m increase (middle graph) and a 250 pF change in the load impedance (lower graph).

This characteristic behavior is used in LIRA to detect any load change, even if the value of the capacity change cannot be measured.

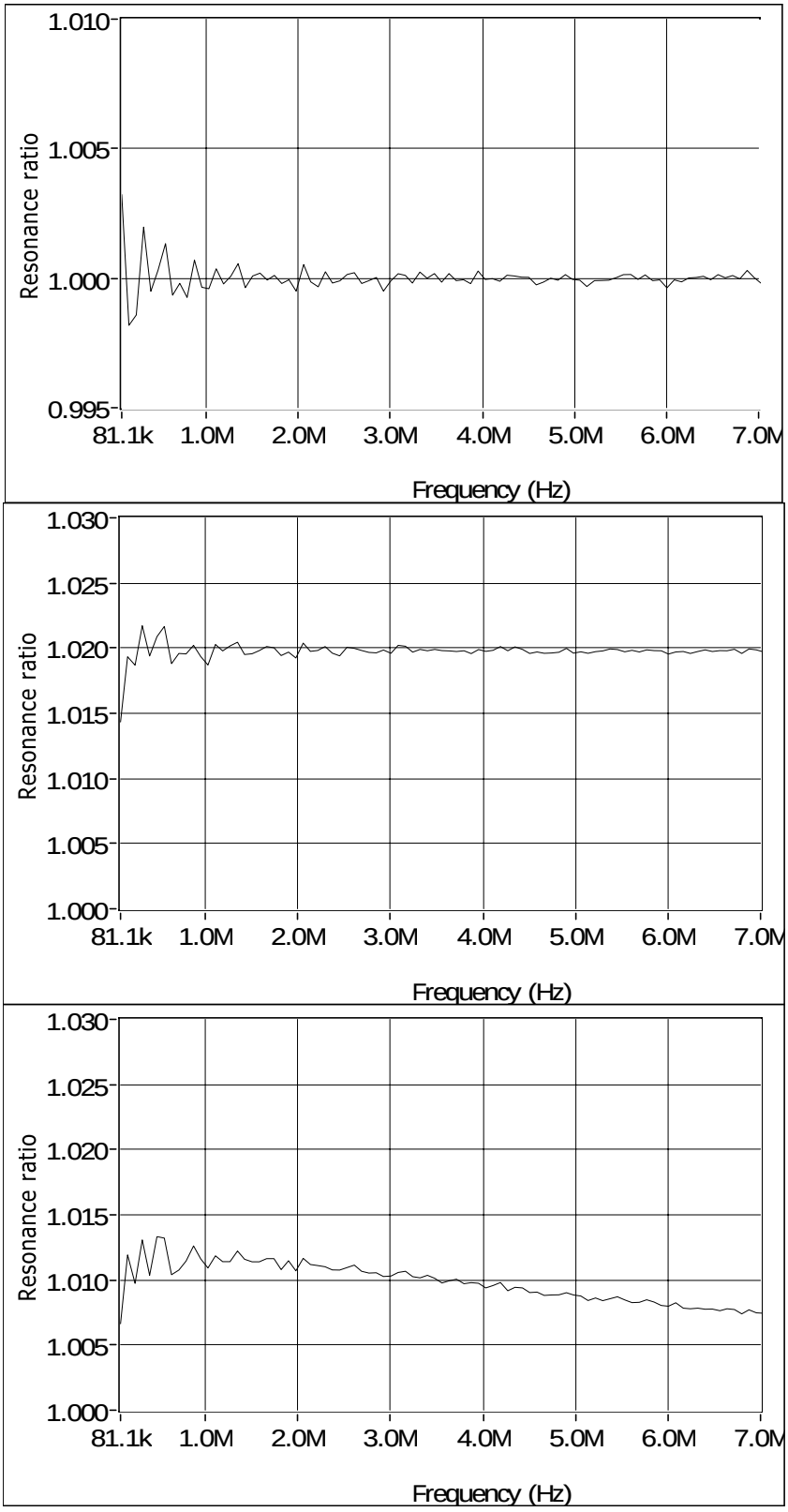

Figure 13. Shift of resonance frequencies vs. frequency

3.2 The LIRA System

3.2.1 Overview

The LIRA system includes a simulator, based on the transmission line theory as explained in paragraph 3.2, which can simulate the behaviour of cables connected to any kind of loads, when excited by an AC source. The cable can be composed by any number of segments, where each segment is characterized by constant values of the 4 electric distributed parameters (R,L,G and C).

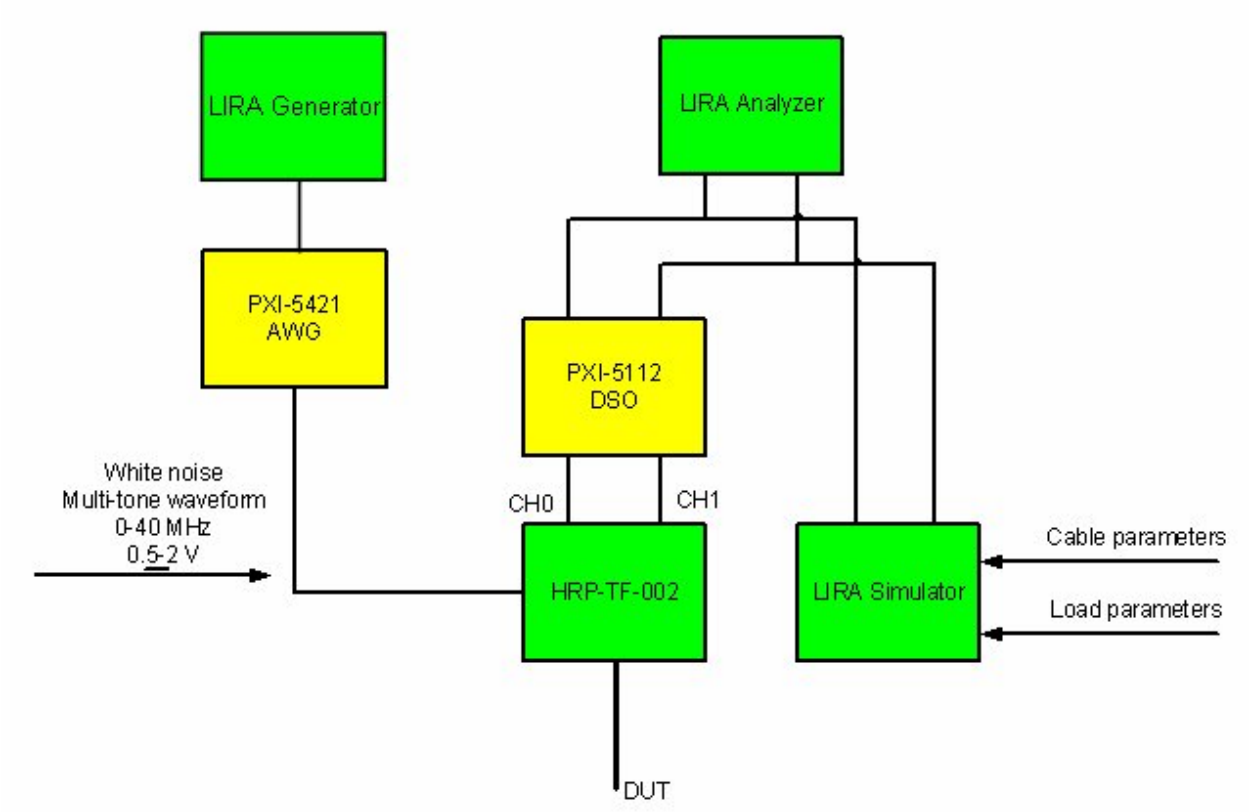

Figure 14. LIRA System Functional Diagram

Figure 14 shows the complete LIRA system. The dark boxes are HRP developed modules; the light boxes are hardware commercial equipment. The building blocks are:

- The **LIRA simulator**. This module can be operated stand alone, or it can be connected to the LIRA Analyzer. In the last case it performs an inverse Fourier transformation to provide the analyzer with the 2 channel time signals, as they came directly from the Modulator Box (HRP-TF-002) connected to the tested cable.
- The **LIRA Analyzer**. It can be operated in real or simulation mode. In the first case it takes the input from the 2-channel Digital Storage Oscilloscope NI-PXI-5112, in the second case the input comes from the LIRA simulator module. The LIRA Analyzer is the core of the wire monitoring system. The operating mode can be switched on the fly during the operation.
  The LIRA Analyzer works both in frequency and time domain [14], performing the following tasks:
  - *Frequency Domain:*

- Estimate and displays the frequency spectrum of the line input impedance.
- Calculate the resonance frequencies.
- Estimate the cable characteristic impedance.
- Estimate the cable length.
- Detect any hot spot and localize it.
- Detect changes in global cable aging
- Detect load changes.

- *Time Domain:*
  - Select one or more resonance frequencies and send commands to the PXI-5421 AWG to generate and supply to the HRP-TF-002 a signal containing only the selected sine waves.
  - Measure and display the amplitude ratio and the phase shift between the 2 acquired channels (CH0 and CH1). The phase shift is initially zero and any deviation from that can be correlated to a change in the cable electric parameters.

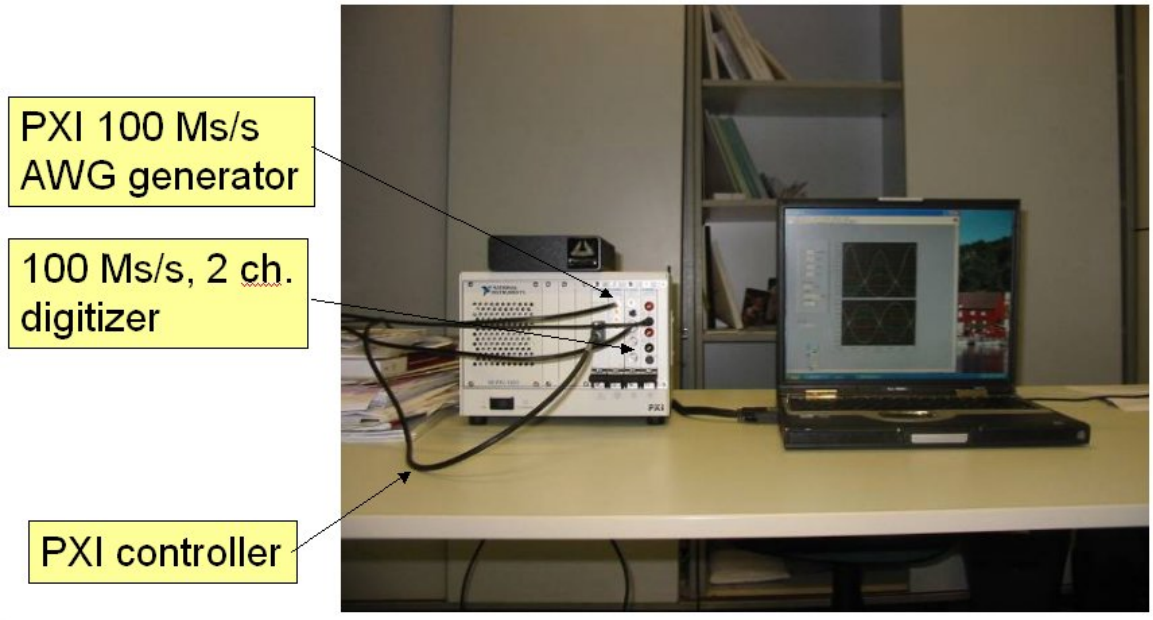

Figure 15. The LIRA System

3.2.2 Reference and Slave channel identification

LIRA is driven by 2 acquired channels (CH0 and CH1), output from a NI-PXI-5112 digital oscilloscope. The signal is generated by a NI-PXI-5421 Arbitrary Wave Generator that, according to the LIRA mode of operation, outputs one of the following waveforms:

- PRBS (Pseudo Random Binary Sequence), for the frequency analysis mode and hot spot detection and localization.
- Multi-Tone Wave: a signal composed of sinusoidal waves of specified frequencies and fixed amplitudes (random phases).

- Chirp signals. This can be used instead of the PRBS signal with increased performance in low noise environment.

3.2.3 The LIRA Simulator

LIRA includes a simulator that solves and uses the equations described in paragraph 3.2. It is then a frequency domain tool producing all the cable variables as a function of the signal frequency.

The required inputs to run the LIRA simulator can be divided in the following categories:

- **Cable parameters**: The simulated cable can be composed of any number of segments, where each segment is identified by constant distributed electric parameters. Each segment can be enabled or disabled to verify the system response to parameter alterations and hot spots. For each segment, the following parameters must be provided:
  - *Length*: The segment length, in meters, can be any number from just few centimeters to several kilometers. Short segments are used to simulate hot spot effects.
  - *Diameter*: it is the conductor diameter in mm. This value is used to calculate the resistance R for unit length (Ω/m) of the conductor, taking into consideration the skin effect at high frequency. R enters in the calculation of the propagation constant and the characteristic impedance. Its value starts to be significant at the highest frequencies and/or longer distances.

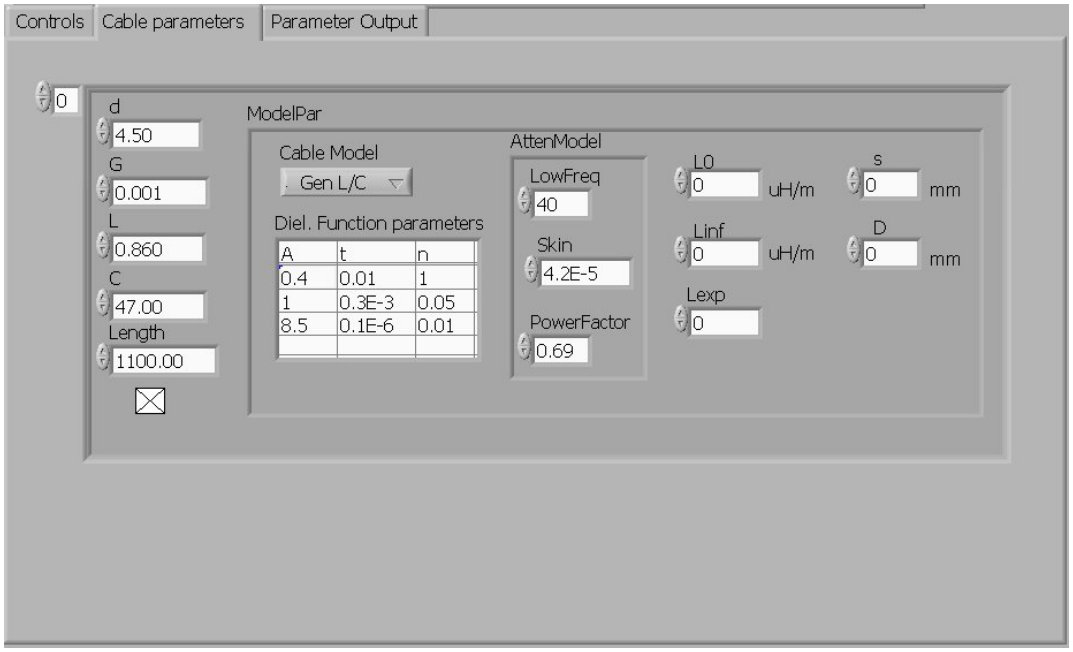

Figure 16. The LIRA Simulator Control Panel

- *Insulation conductivity (G):* this is the conductivity of the insulation material, expressed in *(1/MΩ)·m* and it is significant only at the lower frequencies.
- *Wire inductance (L):* This is one of the two important wire parameters that affect the cable behavior at the higher frequencies. It is expressed in *mH/m.*

- *Insulation capacitance (C):* This is the most sensitive parameter and the one that increases as a consequence of insulation degradation. Its normal value is around 50-100 *pF/m.*

- **Loading parameters:** As explained in paragraph 3.2, the load impedance affects the *reflective coefficient* and then the entire response of the system to an input signal. The load impedance is set as R,L and C.
- **HRP-TF-002 inputs:** These are the inputs used by the system to simulate the effect of the modulator box.
- **Other inputs:** The other inputs are normally left at their default value and they are used to improve the readability of the simulator output (see Figure 20).

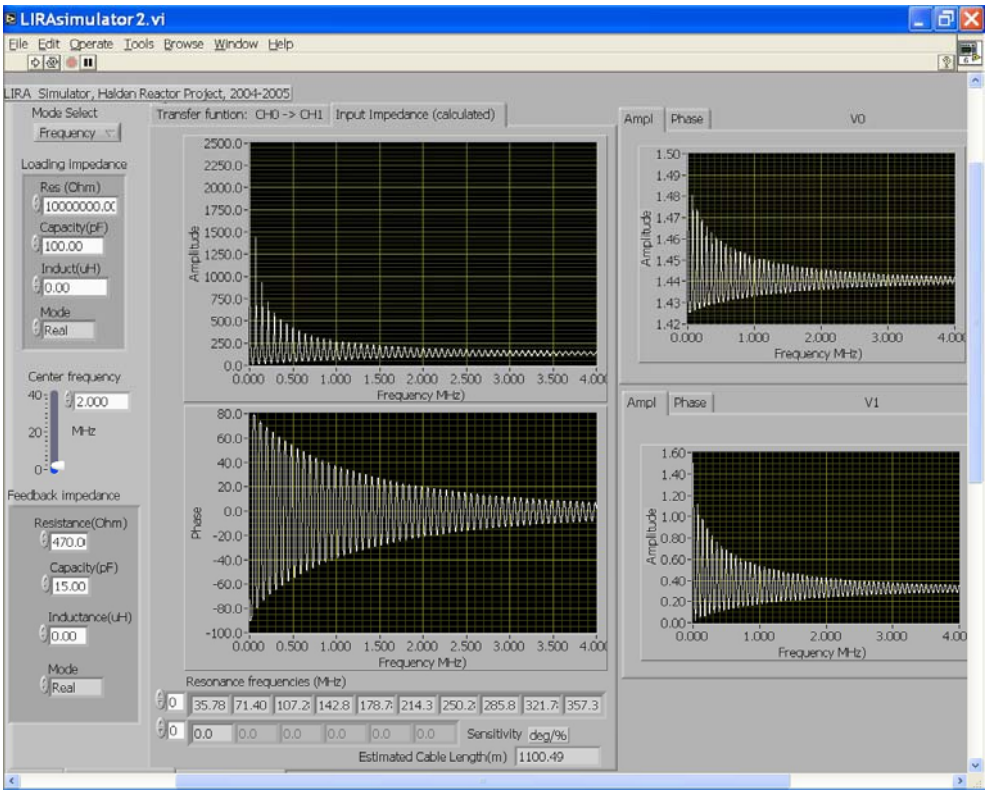

Figure 17. LIRA Simulator Display

Figure 17 shows an example of output display for a simulated cable connected to the HRP-TF-002 modulator box. The two graphs to the left show the frequency spectrum (amplitude and phase) of the line impedance, as it would be estimated and displayed by the LIRA Analyzer for the simulated cable. The graphs to the right show the frequency spectrum of the two channel voltages (CH0 and CH1), inputs to the LIRA Analyzer.

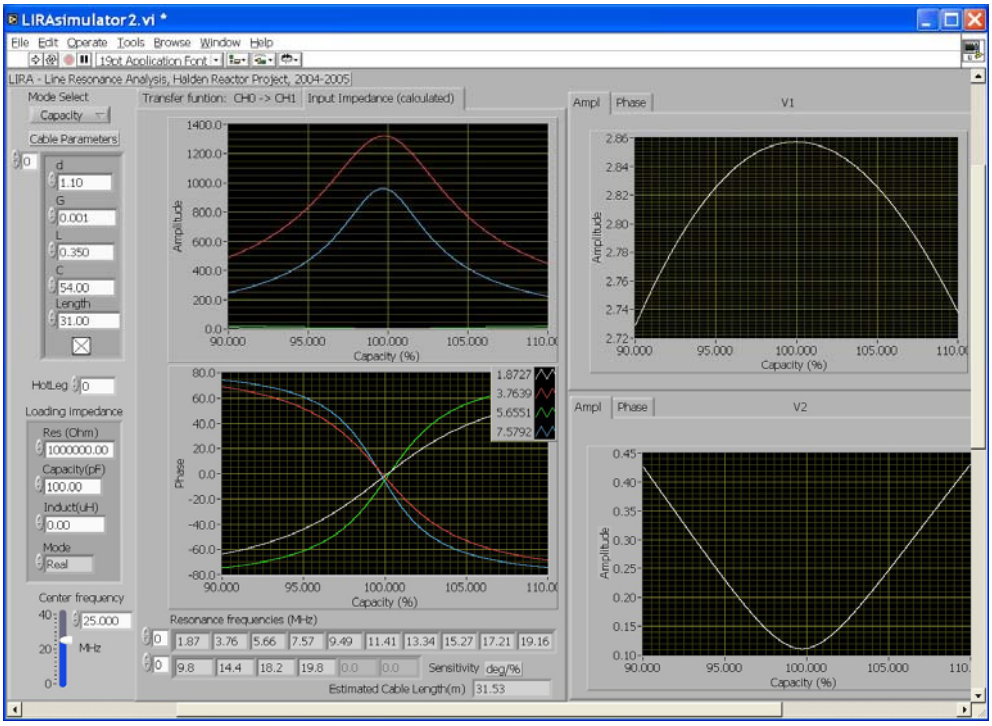

Figure 18. Sensitivity Analysis in LIRA Simulator

The LIRA Simulator can perform also a sensitivity analysis, where the deviation from a resonance condition is plotted against the percentile change of the insulation capacitance. Figure 18 is an example of sensitivity analysis at 4 different resonance frequencies, for a simulated cable.

There is another group of outputs from the simulator that are important for their role in matching the real cable characteristics to the inputs parameters:

- The cable estimated length. This value should match the total length of the cable segments.
- The wire resistance (Ω/km). Plotted against frequency, it is a value normally found in cable datasheets.
- The wire attenuation (dB/km). Plotted against frequency, it is the real part of the propagation constant γ.
- The phase constant (β). It is the imaginary part of the propagation constant γ.
- The phase velocity. It is the speed of the electromagnetic field in the cable medium.
- The phase velocity ratio. Usually found in cable datasheets, it is the ratio between the phase velocity in the cable medium and the light speed in vacuum.
- The characteristic impedance, also plotted against frequency.
- The *load reflection coefficient.*
- The *generalized reflection coefficient*.

The following group of outputs is plotted against the real part of the load impedance:

- Loading sensitivity. It shows how the load resistance affects the departure of a resonance condition for a 1% distributed capacity change (C, pF/m).
- *k-factor*. It shows the coefficient to be used to compare a shift deviation with load L, with the reference deviation at L=∞. That means: $\left|\Delta\phi\right|_{L=a} = kfactor_a \times \left|\Delta\phi\right|_{L=\infty}$. Note that *kfactor=0* when L=Z_0, or when the

load L matches the characteristic impedance of the cable. This explains why the LIRA method cannot be used on-line in matched transmission lines (that is normally not the case of I&C and power cables). For LIRA to be used in matched lines, the load must be disconnected from the cable before the test.

The last, but important, output of the LIRA simulator is the *HotSpot Detector* window. The HotSpot Detector algorithm is like a radar view of the cable from the beginning to the load and it shows any sudden change of the electrical parameters of the wire, providing information about its exact position in meters along the cable from the LIRA equipment. It will be discussed later in this report.

The simulator can be operated as a stand alone program, to study the behaviour of a cable and analyze the sensitivity of any parameter, or it can be connected to the LIRA Analyzer to supply real-time time domain inputs to it. In the last case, the simulator performs an inverse Fourier transformation to produce the required CH0 and CH1 voltage signals to be input to the analyzer. The mode of operation (real/simulation) can be switched on-line at any time, so that it is possible to compare the real behaviour with the simulation in real-time, helping to calibrate the simulator input parameter for that particular cable. Using this procedure, it is possible to get detailed information about the cable under test, information that the simulator provides and that would not be possible to acquire by other means. Other possibilities using this setup include what-if analysis, where anticipated scenarios can be first simulated and then recognized during real operation.

3.2.4 The LIRA Generator

The LIRA Generator provides the signal input to the Box Dispatcher HRP-TF-002, as shown in Figure 14. The generator has been developed to be used with the National Instrument NI-PXI-5421 Arbitrary Wave Generator. Figure 19 shows the generator display with the user controls. The basic feature of the LIRA Generator is its capability to generate the 3 following signals:

1. Pseudo Random Noise (PRN): it is equivalent to white noise, but slightly more stable than that. This signal is used for the frequency domain part of the LIRA System. The amplitude of the signal is user configurable.

2. Chirp signal. An alternative to PRN. Our latest tests show a better performance in terms of S/N ratio.

3. Multi-Tone waveform: A signal composed of the sum of sine waves at selected frequencies. The frequency values can be manually input by the user, but more often they are resonance frequencies generated and automatically input by the LIRA Analyzer.

The operation of he LIRA Generator is completely controlled by the LIRA Analyzer, so that the only thing to do here is to make sure that the PXI-5421 is connected to the HRP-TF-002 and start the generator program.

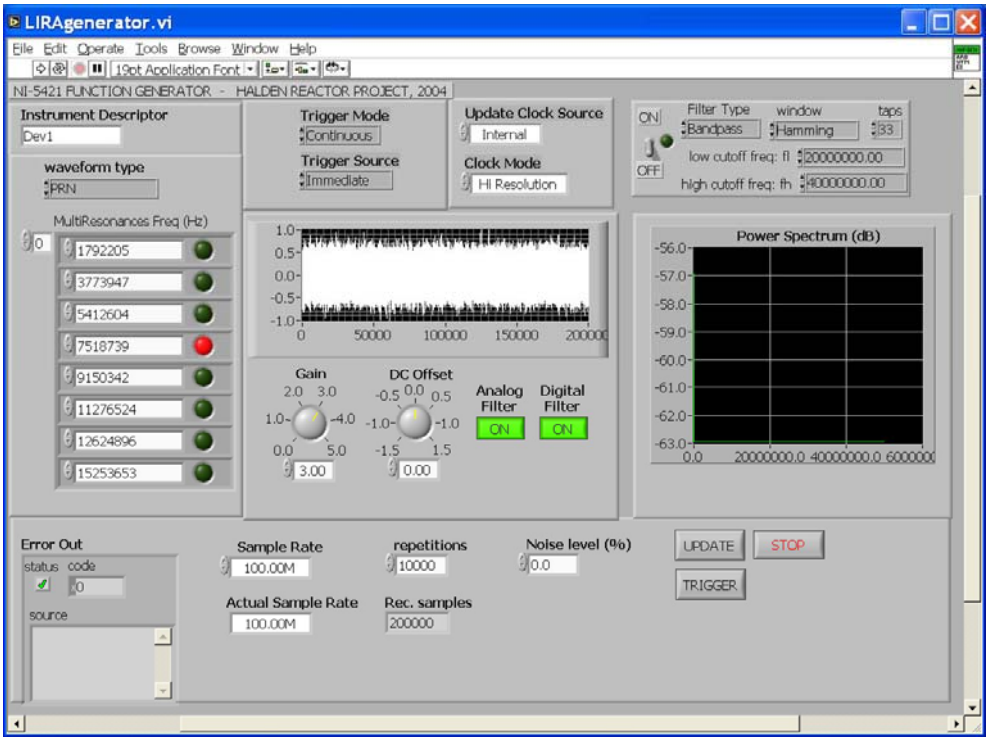

Figure 19. The LIRA Generator

3.2.5 The LIRA Analyzer

The LIRA Analyzer is the core of the LIRA Condition monitoring System. Its purpose is to analyze the two signals (CH0 and CH1) output from the HRP-TF-002 (or the simulated signals from the LIRA Simulator) and provide information about the actual condition of the attached cable. The LIRA Analyzer is much more than an impedance analyzer, because the output from it is not just line impedance as a function of frequency. It is developed to be used with the NI-PXI-5112 Digital Storage Oscilloscope (DSO) from National Instruments, although it can be easily adapted to other DSO models. For our purposes, the PXI-5112 is a good compromise between price and performance: its maximum sampling rate is 100MS/s, which results in a maximum frequency analysis of less than 50MHz (Nyquist frequence).

Figure 20 shows the Control display of the analyzer. The button at the upper right corner is the input selector switch: it is used to switch on-line the input to the system from the simulator to the real equipment and back. The other controls interact with the operation of the PXI-5112 and are usually left at their default value. Three of these controls are worth to be mentioned here:

- The sampling rate: it goes from 0 to the DSO maximum value of 100MS/s. The best operating value depends by the cable length. Long cables have lower resonance frequencies and are better analyzed using lower sampling rates. At this purpose, note that the frequency resolution for spectrum analysis is: $df = \frac{f_s}{r}$, where f_s is the sampling frequency and r the record length. Increasing f without need produces a decrease of accuracy at the lower frequencies.
- The record length: it sets the number of samples to be acquired before the analysis is performed. Increasing the record length results in a higher frequency resolution. Note that the analysis is performed continuously, for each block of data of r samples: at 20 MHz, for example, the time needed for the acquisition of a block of data of 10000 samples is 0.5 msec.

- The data range: it sets the resolution of the analog to digital conversion unit in the PXI-5112. The unit has an 8 bit resolution, so that the maximum digitized value is set to 256. Increasing the data range results in a decrease of accuracy in the digitized signal.

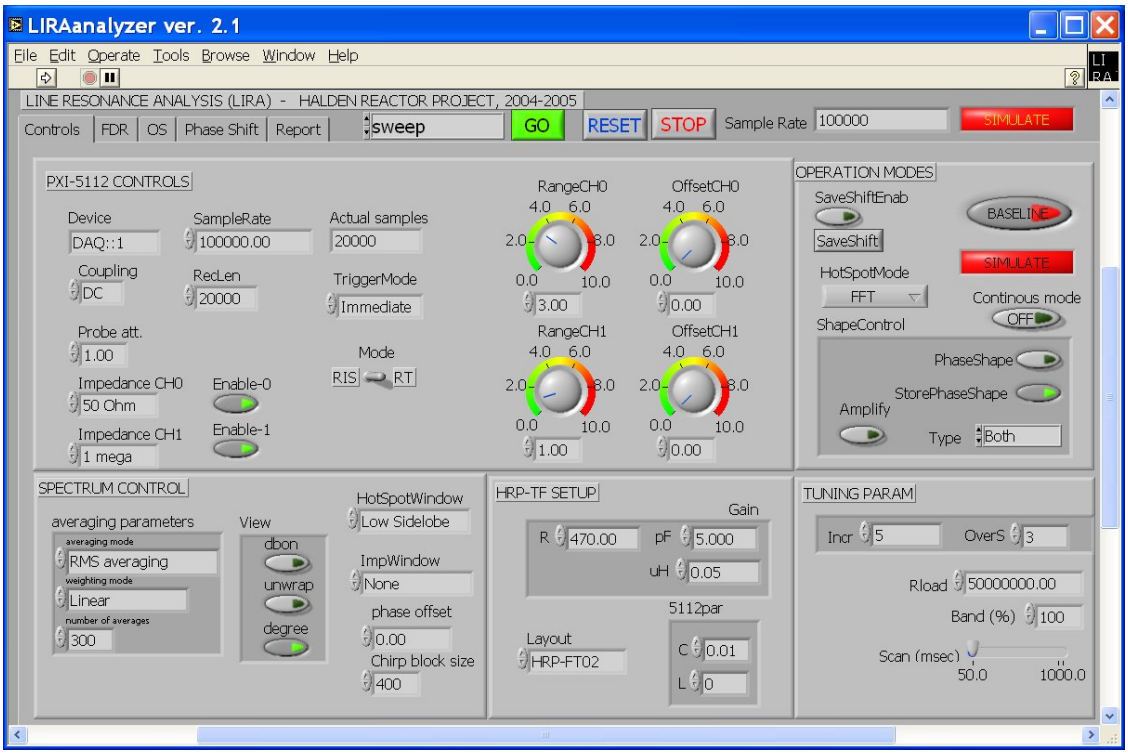

Figure 20. The LIRA Analyzer Control Display

Figure 21 shows the window of the Frequency Domain Analysis module in the LIRA Analyzer. The two graphs to the left represent the line impedance (amplitude and phase), as estimated by the analysis of the PRN signal from the PXI-5421 generator and converted in the CH0 and CH1 signals in the HRP-TF-002. The CH0 (or CH1) signal is visible in the graph at the lower right corner, in Figure 21.

Other information provided in this display includes:

- The resonance frequencies: they will be used for the phase shift monitoring, in the Multi-Tone Waveform Operation Mode.
- The estimated cable length, in meters.
- The estimated cable characteristic impedance.

Figure 22 is an example of HotSpot detection in the corresponding display. This picture is from a real experiment on a 31 meters cable with a local damage at 11 meters from the equipment. This module can diagnose the problem and estimate the position of that with considerable accuracy (10.94m in this example). The HotSpot Detector module will be discussed later in this report.

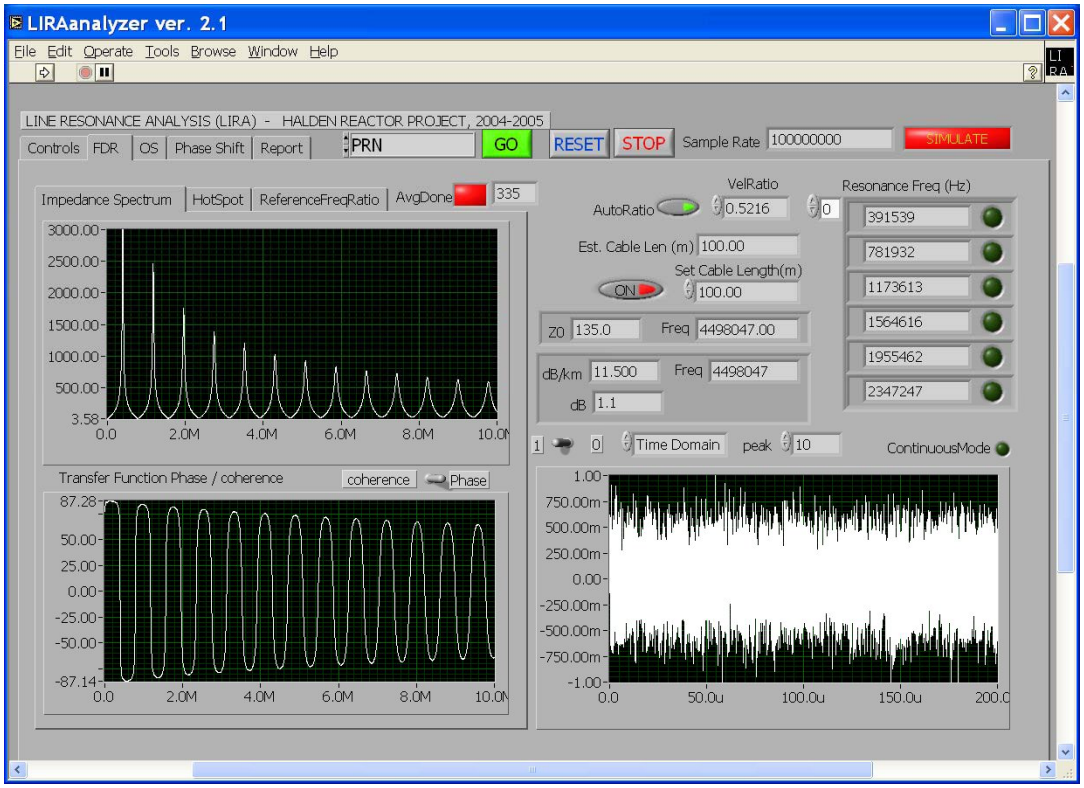

Figure 21. The LIRA Analyzer FDR Display

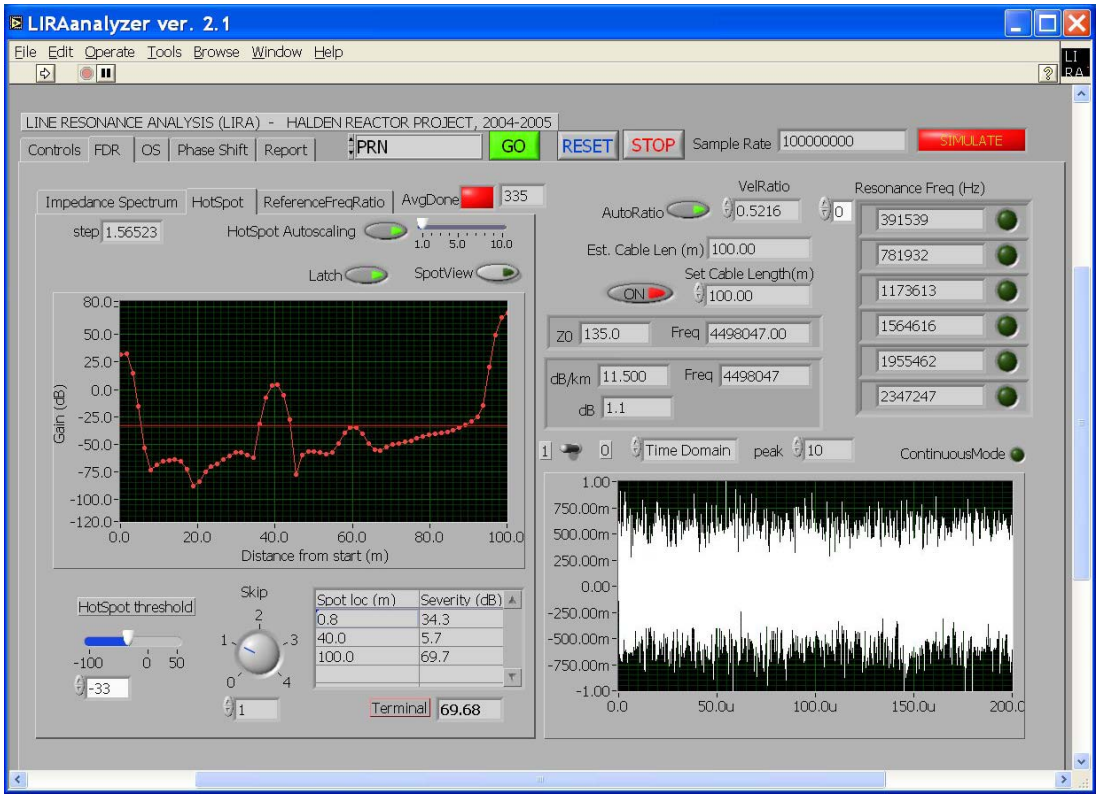

Figure 22. The LIRA Analyzer HotSpot Detector Display

The display for the Multi-Tone Phase Monitoring Mode is shown in Figure 23. Here the graph at the top left is the sine wave generated by the PXI-5421 at a resonance frequency. Note that the signal is clipped at 1.5V because of the range setpoint selected in the control window. This is a normal setup, because of the finer discrimination achievable with no loss of the phase information. The middle graph is the phase shift chart. It represents the phase difference between CH0 and CH1, which is also the phase of the line impedance. This value is 0 at resonance conditions and shift away from that when a local or global perturbation occurs (changes in the cable C or L). In the example shown, only one sine wave has been selected, at the resonance frequency of 7.58 MHz.

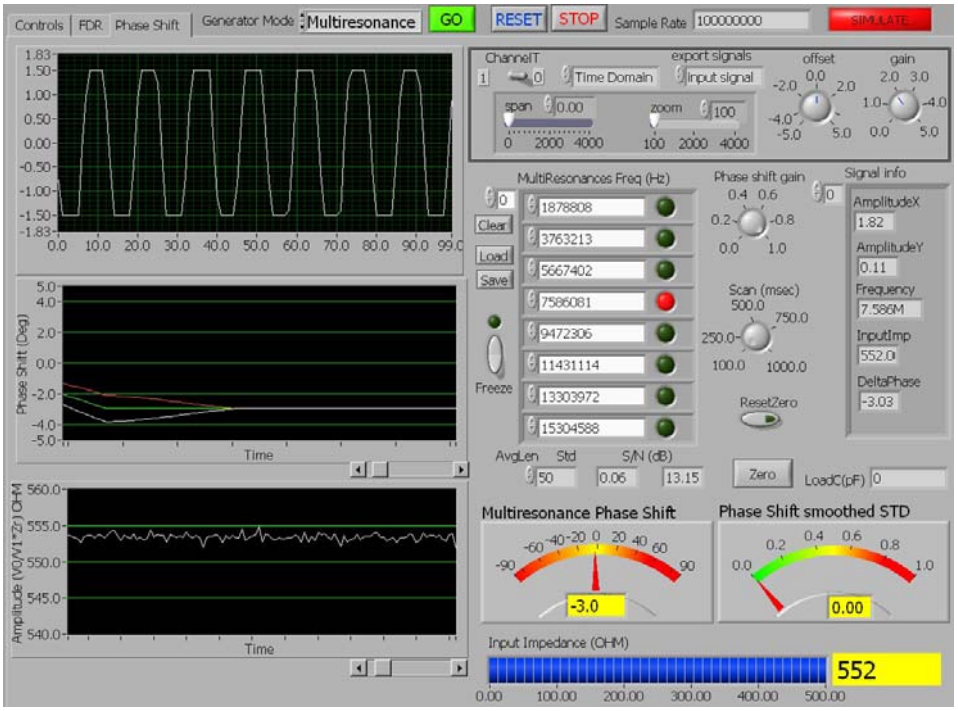

Figure 23. The LIRA Analyzer Phase-Shift Monitoring Display

4. ASSESSMENT OF CABLE DEGRADATION WITH LIRA

4.1 Overview

Extended field tests must be performed in order to assess the capability, sensitivity and limitations of the LIRA System. The objectives of cable tests can be stated as follows:

- Assess the accuracy of the LIRA Simulator. This goal can be achieved by comparing real test results with corresponding simulated tests, performed with simulated cables of the same type, condition and length. Simulator tuning and assessment is an important step, because the simulator provides information and results not achievable otherwise. In addition to that, the simulator can be used to extrapolate the cable condition and predict its future behavior.

- Assess the correlation of the phase-shift indicator to the cable condition (degradation state). Simulated tests can provide information on the correlation between impedance phase and wire electric parameters (L and C). The final goal is deriving a curve for each cable type of interest, correlating the phase to the degradation state. An additional important goal is the determination of the correlation between the phase indicator and another accepted condition indicator, namely the elongation at break (EAB)[2,3].

- Assess the capability, sensitivity and accuracy of LIRA in the detection of hot spots (localized cable degradation).

At the time of writing, the following tests have already been performed and analyzed:

- Tests on a PVC, I&C twisted pair cable installed at the Halden Reactor, 100 m
- Tests on EPR and XLPE cables, 16-50m, in co-operation with EPRI.

LIRA provides 2 condition monitoring indicators that can be used for the assessment of an installed cable:

- The *line impedance phase shift.*
- The *HotSpot Detector* signature.

The first indicator is used both for local and global aging assessment. In global assessment, it must be used together with a baseline condition that is considered the reference point, or initial condition of the cable. For local fault detection, the 2 indicators work together, where the *phase shift* is used as a real-time early warning of a developing fault and the *HotSpot detector* quantifies and localizes the fault along the cable. The next two paragraphs describe in details this mechanism.

4.2 Global Degradation Assessment

LIRA gives an accurate estimate of the phase difference between CH0 and CH1, which is proportional to the line impedance phase at the cable input. This value is zero at any resonance frequency and since the system is setup to operate at one or many resonance frequencies at the beginning of the operation, LIRA can provide information about the cable behavior and condition only from that time and afterwards. In other words, the LIRA phase-shift indicator can assess the global cable condition change from a reference point, also referred to as a baseline.

The line impedance phase and its shift from the resonance is tracked in real-time (see for example Figure 23) and the way it is implemented in LIRA makes it an extremely sensitive indicator of any small change in the distributed electrical parameters (L and C), which in turn are reliable indicators of insulation degradation. The sensitivity of this indicator depends by the following 2 factors:

- The length of the cable (through the operating frequency)
- The type of termination load (see par. 3.1.4)

The dependence by the cable length is shown in Figure 28, for a RG-58 coaxial cable, open end. From this graph it is easy to see that a cable of 100m length, for example, experiences a 250 deg shift for 1pF/m change in the distributed insulation capacitance. Simulated tests show that, even with a background noise of 10% of the signal input, changes down to 0.05 pF/m can be reliably detected and measured in cables of that length.

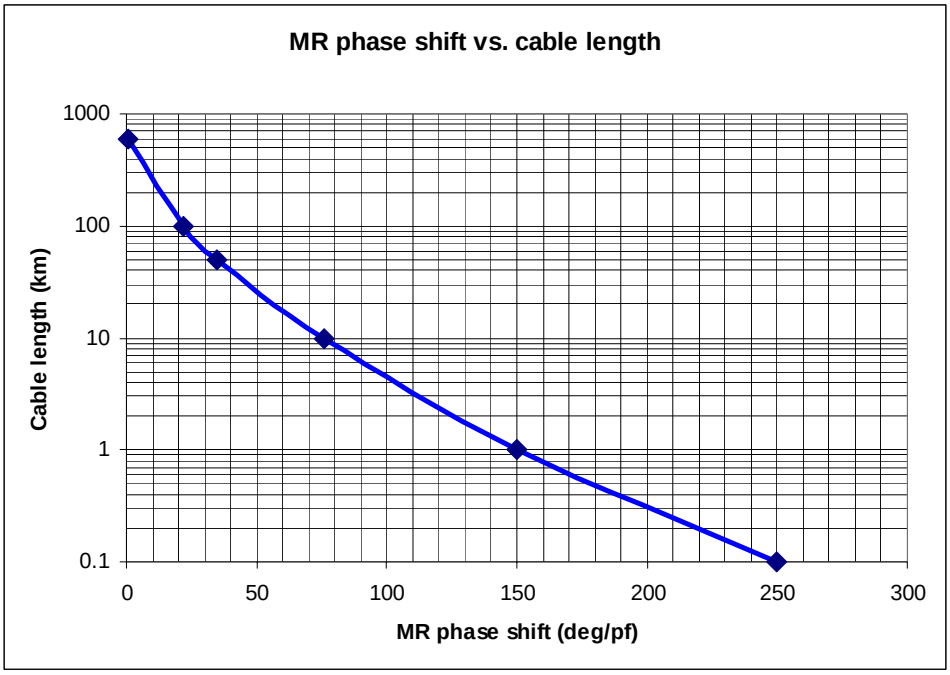

Figure 28. Phase-shift sensitivity to cable length

The reason why the phase shift sensitivity decreases with cable length is the attenuation. Long cables have higher point-to-point attenuation and since the cable losses increase with $\sqrt{f}$ (see Figure 4), the operating signal frequency must be decreased accordingly to maintain resonance conditions in the line. The ultimate effect of a decrease in frequency is a corresponding increase in the signal wavelength and then a diminished response of the phase to parameter changes.

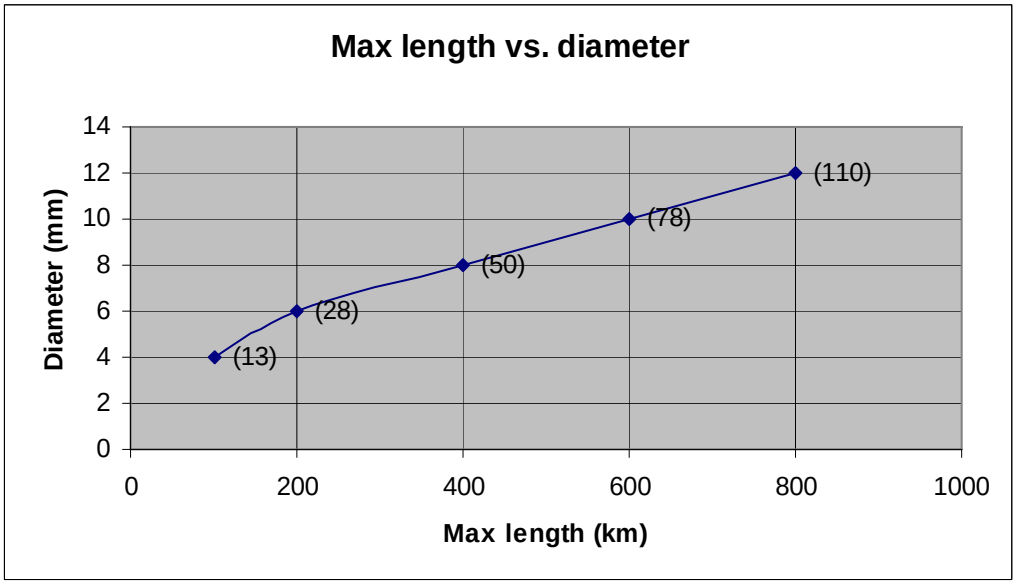

Figure 29. Maximum lengths vs. wire diameter for a typical subsea cable

Figure 29 shows the limits for a typical subsea cable as a function of cable diameter. Although nuclear plant cables are much shorter than the maximum allowed length, applications in other industries (oil&gas for example) might be limited by cable attenuation considerations.

The termination load has an important effect on the shape of the impedance phase. The capacitative effects have been discussed in par. 3.1.4, but the resistive value of the load has a significant impact on the phase sensitivity. Figure 30 shows how the load value affects the phase shift sensitivity in a 100m cable with a characteristic impedance of 125 Ω. This result poses an important limitation to the use of FDR methods for condition monitoring, which can be expressed as follows: "Line resonance methods make use of cable behaviour in mismatched conditions, i.e. when the load value does not match the wire characteristic impedance. If the load matches the line, no resonance is visible". In industrial applications outside the microwave and antenna systems, this is actually a theoretical limit, because the loads applied to I&C and power lines are usually much higher than the relatively low line characteristic impedance, which is usually in the range 50-150 Ω. However, diagnosis on matched lines can be performed only with disconnected terminals (infinite or zero load).

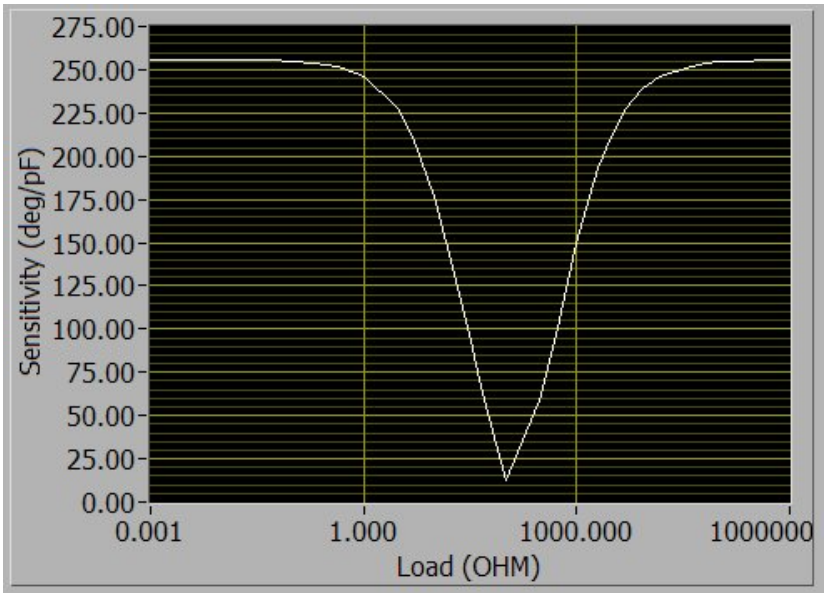

Figure 30. Phase-shift sensitivity to the termination load

4.3 EPRI Tests for Hot Spot Detection

A test in co-operation with EPRI was conducted in USA on September 13th and 14th, 2005, on 10 cable specimens widely used in operating nuclear power plants. These specimens had gone through a global and local accelerated aging process, as summarized in table 1 and 2.
Figure 31 and 32 show the LIRA display for the Okonite specimen in normal conditions. The drift of the line impedance phase towards the negative side is due to parasitic effects at high frequencies, but it has no effect on the spot detection.

Table 1. Okonite (EPR/CSPE) sample parameters matrix

Spec	Bulk Aging (150 C)	Local Aging (150 C)	Length (m)	Spot Location (m)	
OKA	Unaged	None	24.4	None	
OKB	Unaged	329.5 h	16.8	3	
OKC	122 h	None	16.8	None	
OKD	122 h	292 h	16.8	9.1	
OKE	122 h	483 h	16.8	6.1	

Table 2. Rockbestos (XLPE/CSPE) sample parameters matrix

Spec	Bulk Aging (150 C)	Local Aging (150 C)	Length (m)	Spot Location (m)
RA	Unaged	None	24.4	None
RB	Unaged	995.5 h	18.3	3
RC	122 h	None	18.3	None
RD	122 h	1000.5 h	18.3	9.1
RE	122 h	1433 h	18.3	6.1

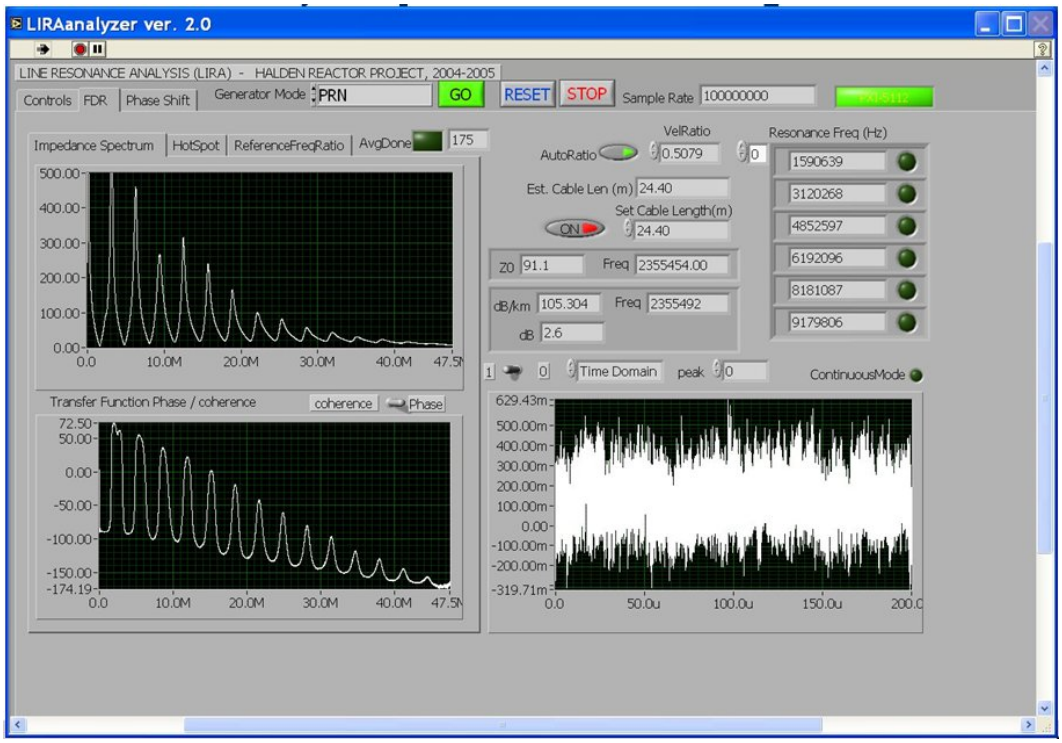

Figure 31. Line impedance of 24.4m Okonite in normal conditions

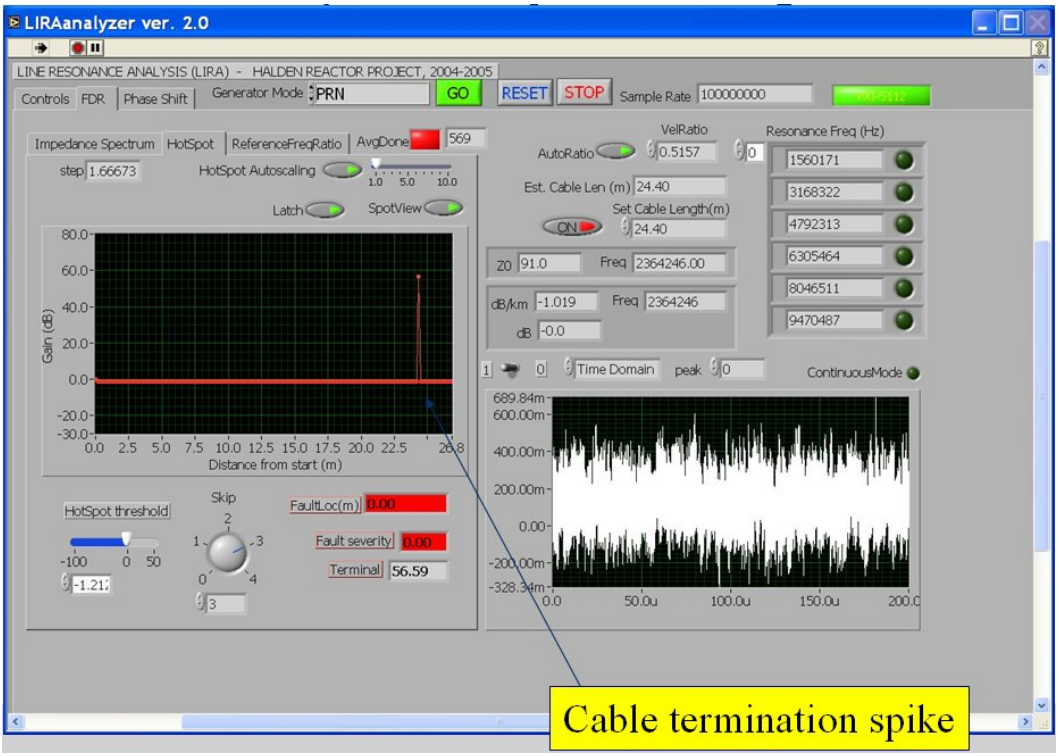

Figure 32. Spot detection trace for Okonite, normal conditions

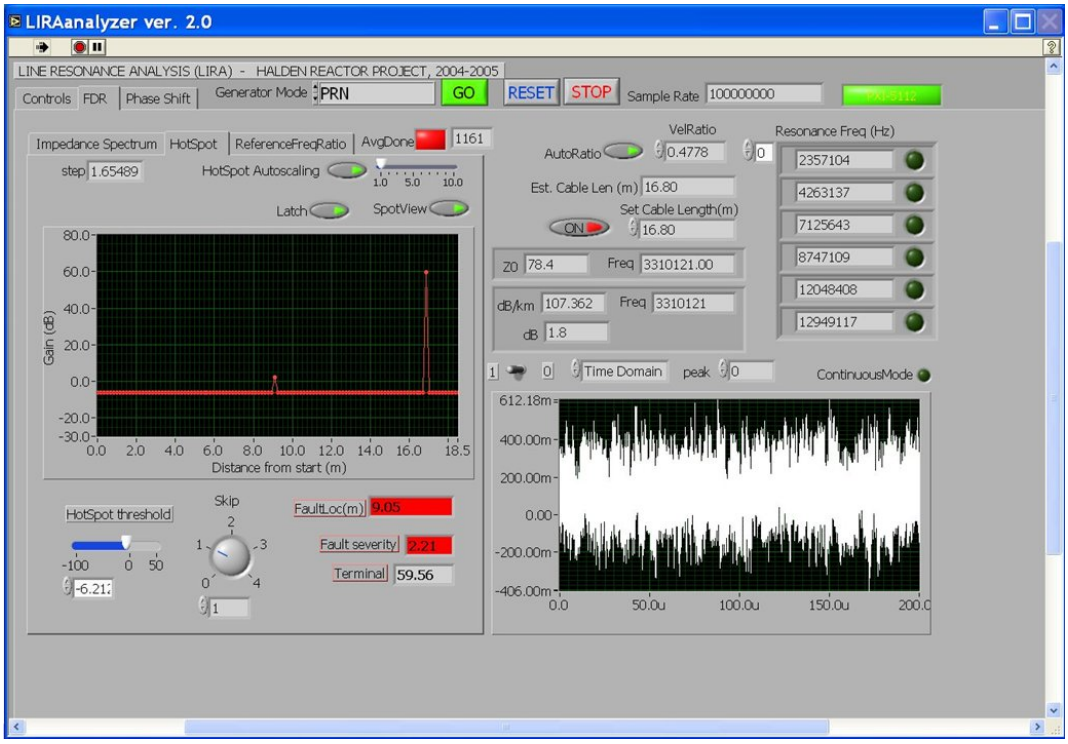

Figure 33. Spot detection trace for Okonite with a local thermal spot at 9.1m

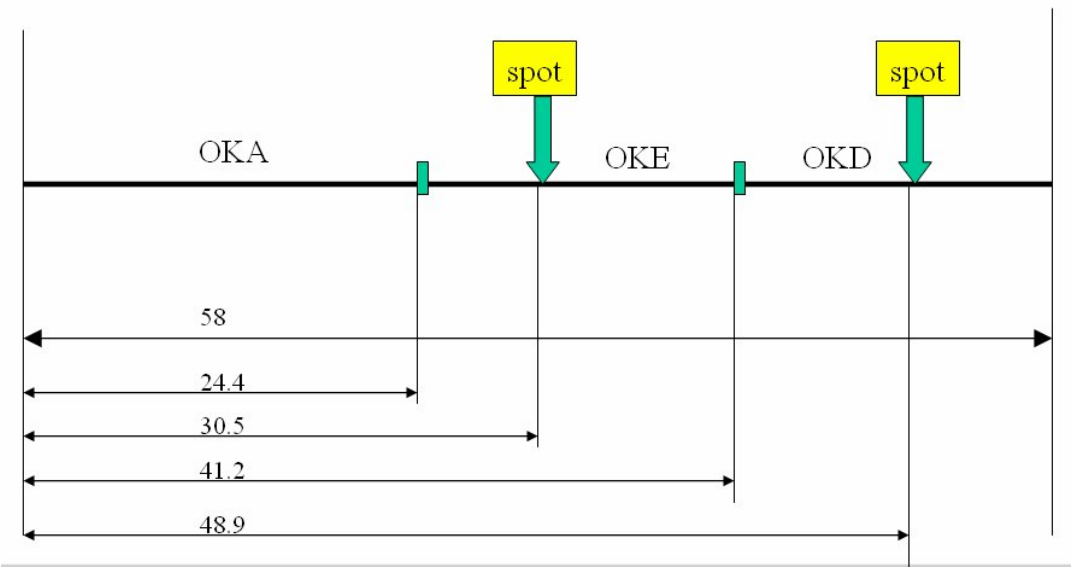

Figure 34. Layout of 3 Okonite connected specimens with 2 hotspots (58m total length)

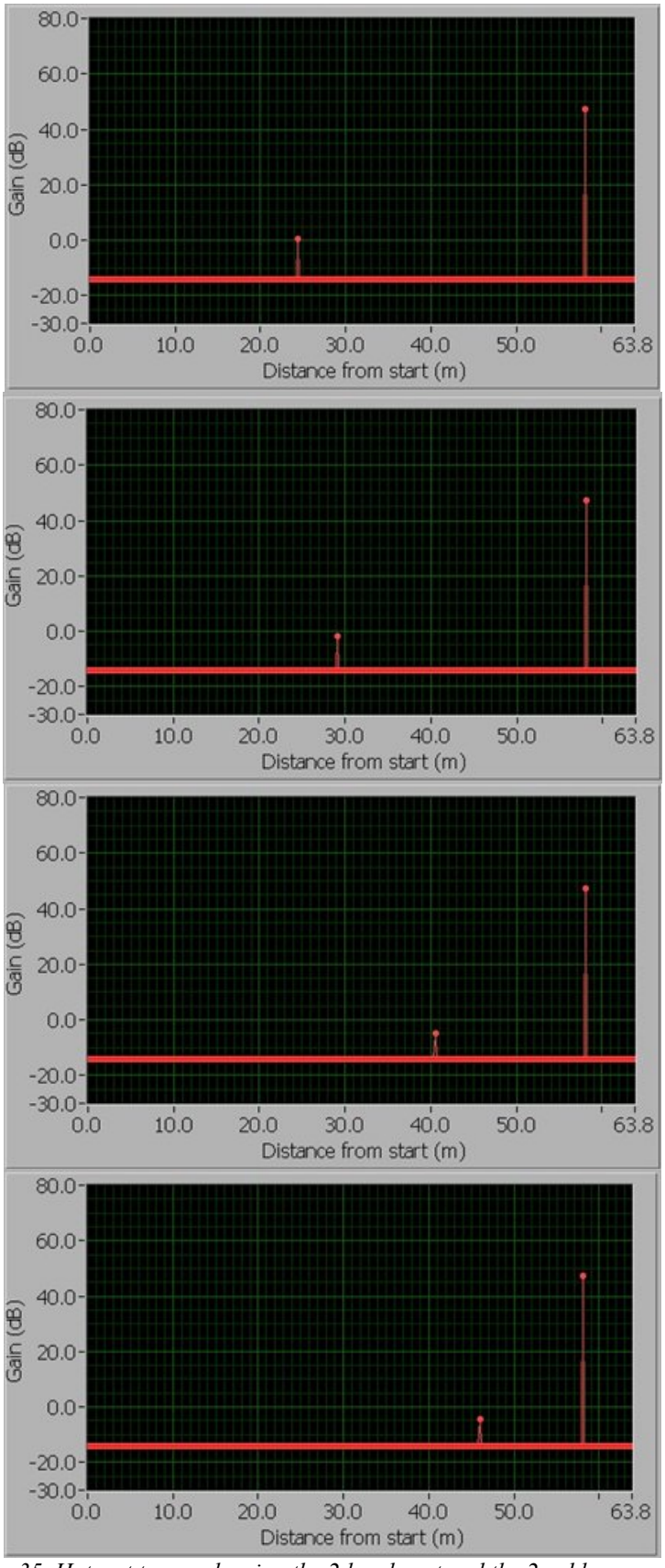

Figure 35. Hotspot traces showing the 2 local spot and the 2 cable connections

Figure 33 shows the result from the measurement of the specimen OKD, where a thermal spot (about 20cm) was present at 9.1m. This hotspot was not detectable by visual inspection and it can be considered the initial local degradation of a cable locally exposed to abnormally high temperature. The localisation error was just 5cm.

To evaluate the impact of several connected cables with multiple hotspots, a layout as in Figure 34 was prepared, where the specimen OKA, OKD and OKE were connected together. Note that while OKA was a not aged segment, both OKD and OKE were globally aged as described in Table 1.

Figure 35 shows the LIRA traces detecting both the connections and the two hotspots at the right position. LIRA cannot discriminate connection spots from thermal spots, so that the knowledge of the cable layout is needed to perform a final diagnosis.

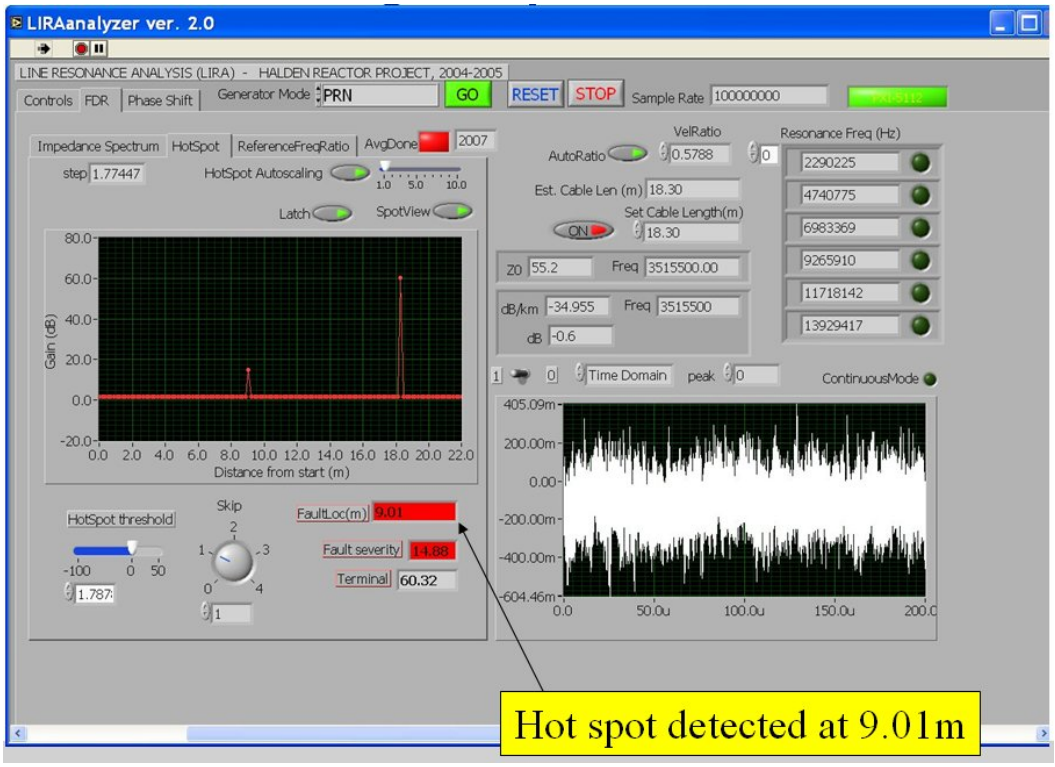

Figure 36. Hotspot detection in the Rockbestos specimen

The Rockbestos specimen gave similar results. Figure 36 shows the hotspot detection for the specimen RD, with a thermal spot at 9.1m.

4.3.1 EPRI Tests Conclusions

LIRA performed well in detecting hot spots in both Okonite and Rockbestos cables, with the exception of the spots too close to a termination, where higher sampling rates would be needed, to increase the resolution.
The localization error is about 0.5%, increasing when aged and unaged cables are connected together and/or the spots get closer to a termination. The accuracy would increase with higher sampling rates.

4.4 Halden Reactor Tests on Installed Cables

LIRA tests were performed in January 2006 on several installed power cables (PVC insulation) at the Halden Boiling Water Reactor (HBWR). The cable state was unknown, all the tested cables have been in service for about 40 years. Measurements were taken with termination open, shorted and connected to the pump motor.

The importance of this test consists in the evaluation of the possible impact of the environment, because this was the first LIRA experiment performed on installed cables. Figure 37 shows the layout of one of the tested cables, 170 meter long.

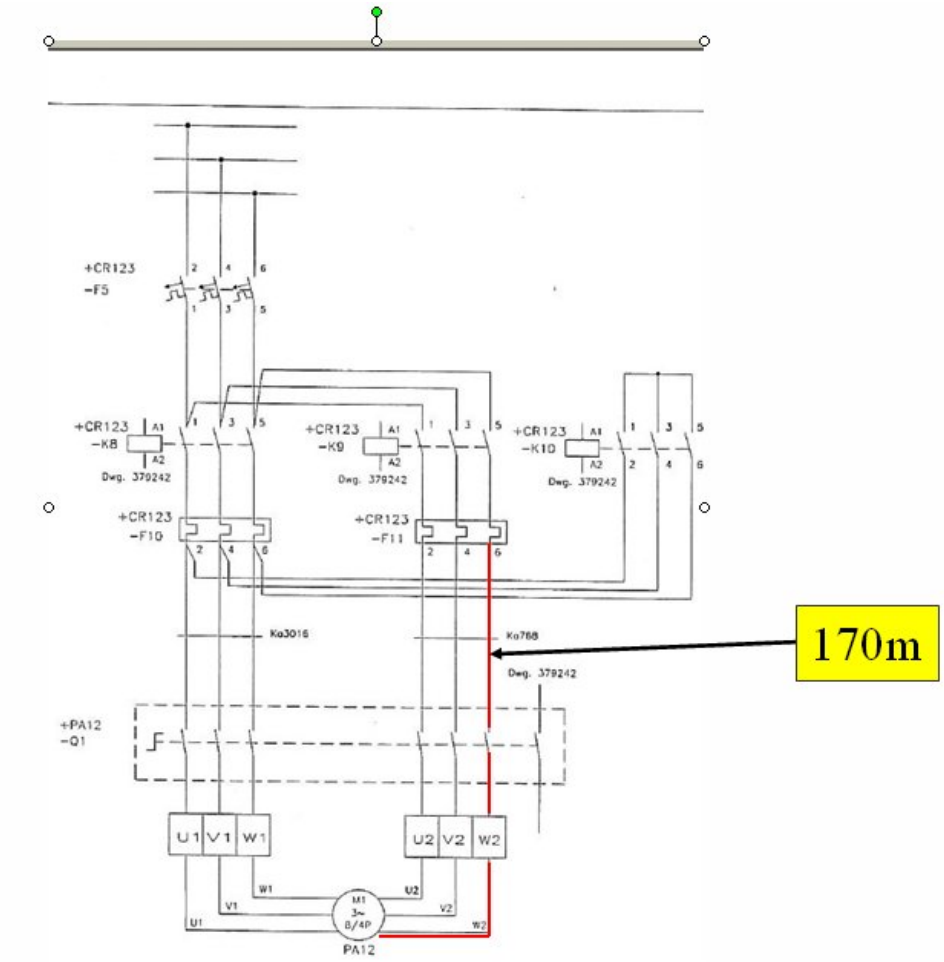

Figure 37. Cable layout for the HBWR experiment

Figure 38 and 39 show the result of the measurements on this cable. The regular shape of the line impedance suggests that the system had no particular influence from the changing environment along the cable.
The spot detection display shows a background level below -60dB, as in simulation tests, except for the first part at the left, which is drifting up as a consequence of the long probes (about 2 meter) used to connect LIRA to the cable. It is not known at this time the reason for the spot visible at 43m from start. Visual inspection of the cable could confirm the existence of a thermal hotspot or a different kind of degradation.

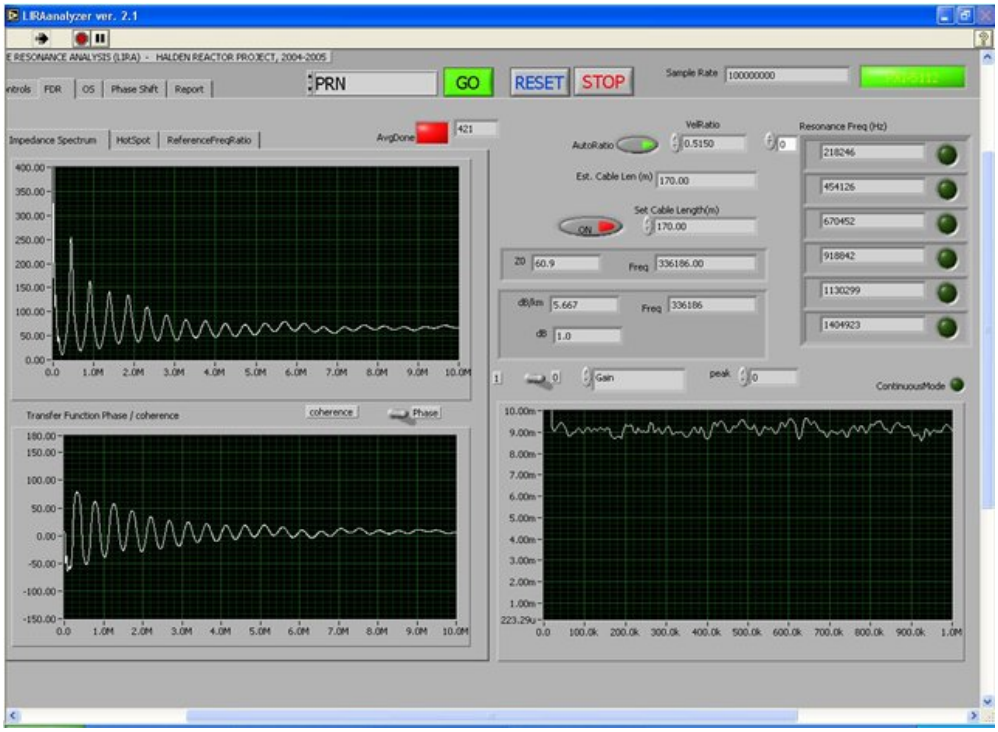

Figure 38. Line impedance spectrum (HBWR experiment)

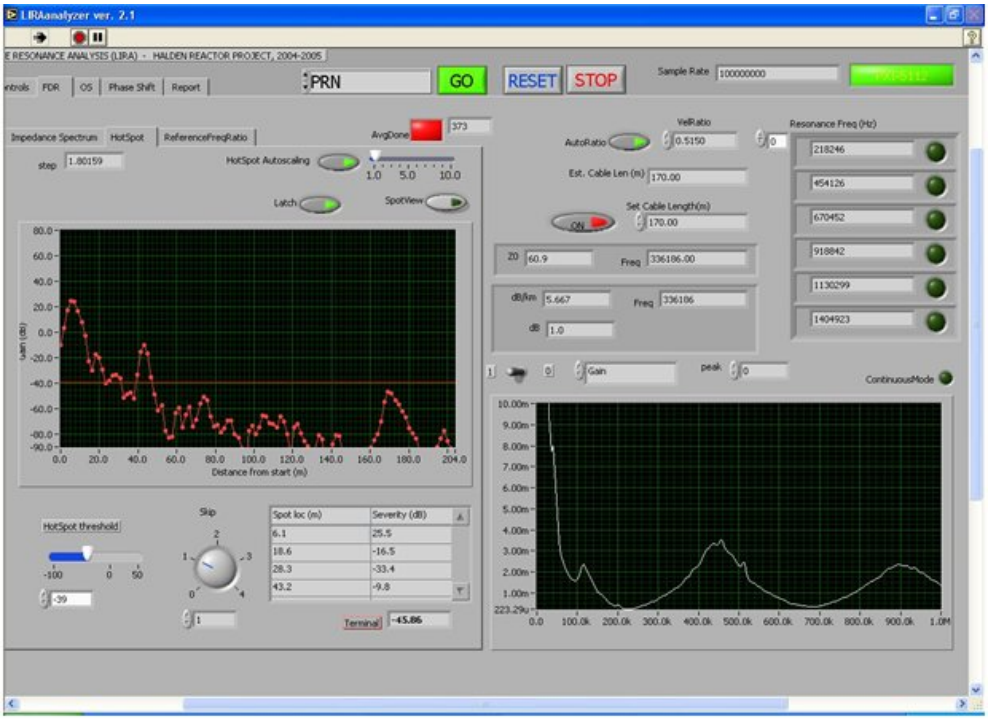

Figure 39. Hotspot analysis (HBWR experiment)

4.4.1 Considerations on the HotSpot Detector analysis

The experiment described in the previous paragraph and its simulated extensions led to many important considerations and conclusions that can be summarized as follows:

- No reference or baseline is needed to perform hot spot diagnosis. No information about the cable is required, like insulation material, electric properties, length.

- Diagnosis is independent by the load characteristic. Capacitative or inductive loads, high or low resistive loads make no difference for hot spot diagnosis.

- Changes in cable inductance and capacitance are additive. There is no compensation effect. Tests on accelerated aging cables show that damage due to high thermal conditions (dry or wet) produce an increase in the insulation capacitance and a decrease of the wire inductance (mainly due to structure changes). Both effects add up in the HotSpot Detector display.

- Shadow zones hide hot spots in the vicinity of the cable terminations. Shadow zones do not depend by the cable length, so they become to be less significant above ~30 m length. Higher frequency analysis make the shadow zones narrower.

- Simulation of the performed experiment shows that hot spots can be reliabily detected when C and/or L changes of about 10 pF/m and/or 0.2 uH/m occur as a consequence of degradation (either dry or wet). After the performed test, cable properties showed 85 pF/m increase from normal.

– Catastrophic cable failures (melt down due to high temperature at 150 °C) can be prewarned (10min in this experiment). Lower temperatures would produce slower, but detectable, effects.

– Hot spot conditions in fully operational cables can be detected and localised. Localisation error is about 1% or less. The impedance phase monitoring, performed continuosly in real-time, is used as an early warning that something abnormal is happening, the HotSpot Detector is run on demand to assess and localize the hot spot.

– Multiple hot spots can be diagnosed and localised with no difference respect to the single spot case.

– Higher frequencies result in much better fault detection and localization accuracy. Even when time domain phase shift analysis recommends resonance frequencies lower than 1 MHz (>10 Km cable length), hot spots analysis takes benefit by spectrum ranges from 0 to 20 MHz also for very long cables, resulting in finer mesh and detection capability (when possible because of the cable attenuation).

4.5 The condition monitoring process

The condition monitoring process involves the following 3 steps:

1. Estimate the current value of the Condition Indicator CI (in LIRA this is the line impedance phase shift and the HotSpot spike size (for local degradation), produced by the compound change of the distributed capacitance C and inductance L).

2. Correlate the CI value with a measure of the global or local cable degradation state.

3. Estimate the residual life of the cable, given the current degradation trend and the applicable qualification criteria.

The LIRA system currently performs the actions in step 1, both for local and global degradation. Although it has been demonstrated that insulation degradation due to thermal aging produces significant and measurable changes in the cable electric parameters, the correlation among these parameters (or the LIRA condition indicators) and the wire condition (that is its ability to perform the task for which it has been installed), depends by many factors and parameters. The list of cable parameters affecting this correlation is as follows:

- Cable structure (coaxial, twisted pair, how many wires)
- Insulation type (this influences the initial value of L and C)
- Cable length
- Cable characteristic impedance
- Type of load connected to the cable (for on-line monitoring)
- Signal frequency. Higher frequencies results in higher sensitivity to electric parameter changes.

For local degradation detection (hot spot detection), the following parameters should be added:

- Fault location. Faults localized near the LIRA equipment have a larger effect than faults close to the cable termination.
- Fault size (along the cable). This is obviously an unknown parameter that can be checked only after visual inspection of the cable. The spike amplitude increases however with the square of the cable length affected by the hot spot. Any degradation assessment should be given relative to the creep size.

These parameters should enter a correlation, together with the LIRA condition indicators, to produce a measure of the current cable state. This process (step 2 of the condition monitoring process), should be performed by an Artificial Intelligence System like the one shown in Figure 40.

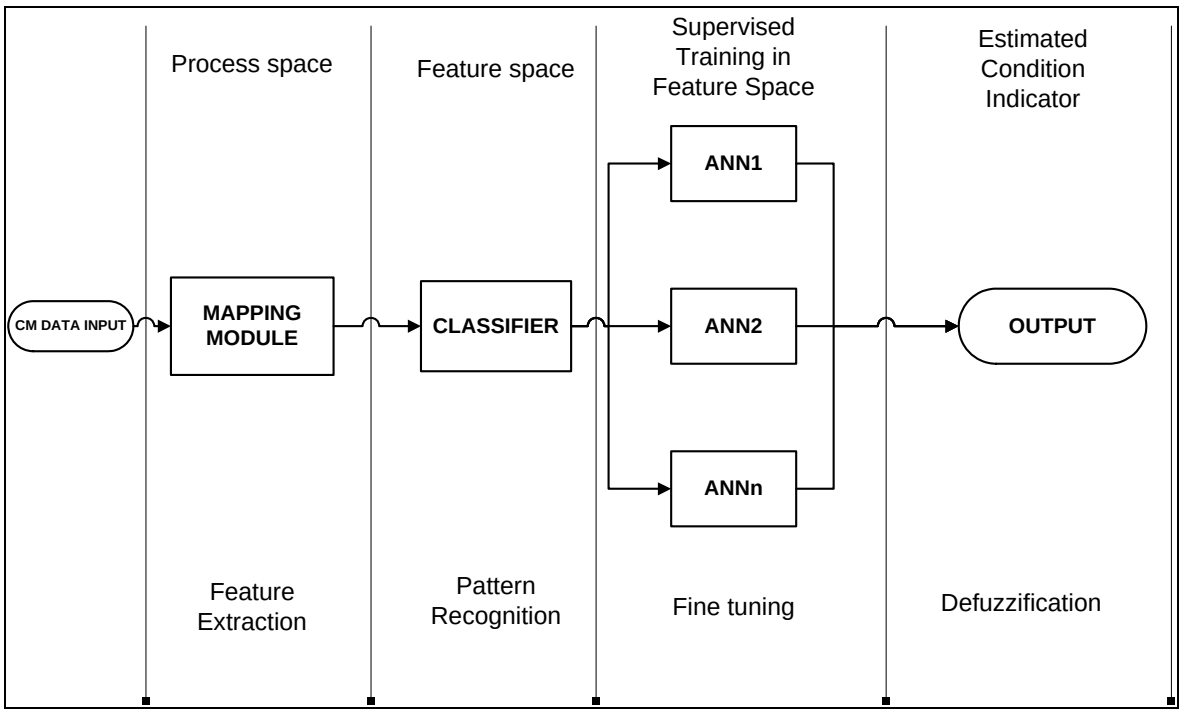

Figure 40. Estimation of the CI using Artificial Intelligence methods

Here, the data input vector includes the line impedance phase shift, the HotSpot spike value and all the parameters listed above. The system classifier and the Artificial Neural Networks (ANNs) blocks must be trained using data from real experiments and from the LIRA Simulator, so that for each input vector a numerical value is produced, corresponding to the current cable condition. This numerical value should be consistent with other accepted condition indicators like the Elongation At Break (EAB), where Figure 41 shows an example of correlation.

It must be noted that the LIRA condition indicators are already excellent signals for early warnings of abnormal or degraded cable conditions. The addition of a module performing the step 2 activities would give a quantitative measure of the corresponding cable state, comparable with other currently accepted indicators that are not usable on-line and cannot detect local abnormal state along the entire length of the cable.

The activity in step 3, residual life prediction, involves some assumptions about the behavior of an insulation material in harsh environments. This assumption could be the validity of the Arrhenius relation [4], stating the correlation between degradation and temperature. Using this assumption it is possible to anticipate the long term behavior of an insulation material under harsh environment condition by accelerating its aging. Accelerated aging is typically performed at temperatures in the range 80-120 C, with acceleration factors of 200 or more. Using these curves, as shown in Figure 42, it is possible to extrapolate the long term values of a condition indicator and estimate the time left before reaching the limiting condition.

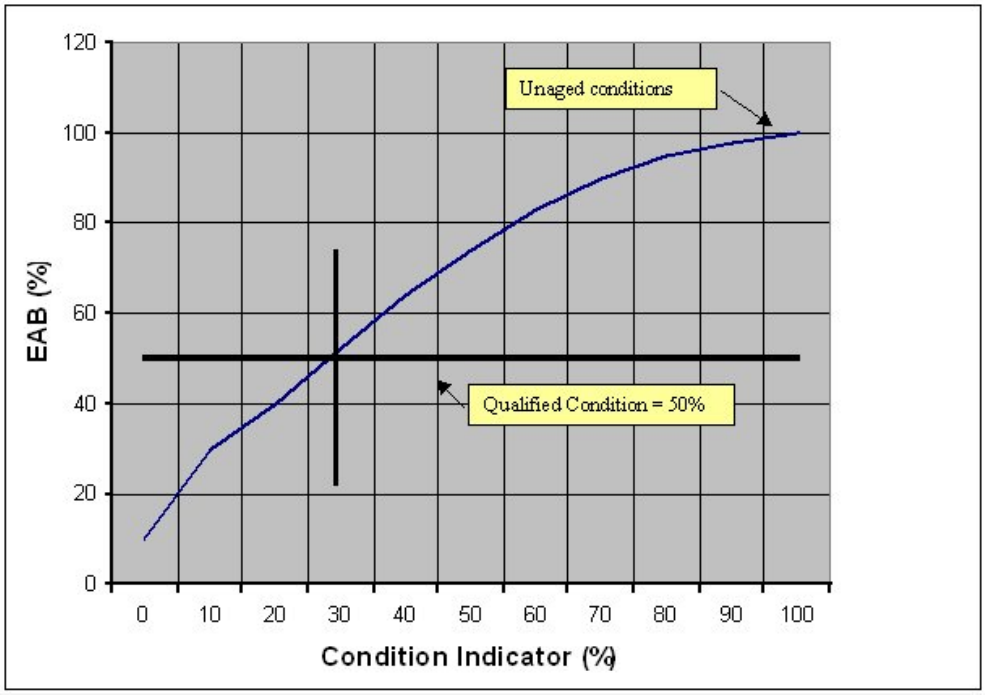

Figure 41. Correlation between EAB and another CI (example)

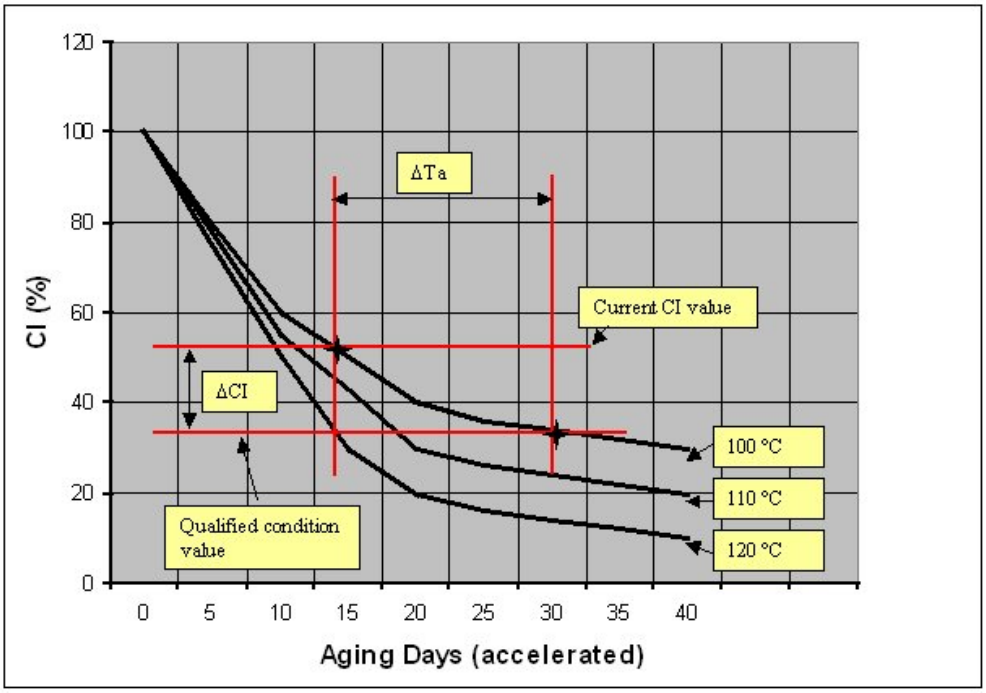

Figure 42. Predicting the cable residual life through Arrhenius relation

5. PULSED POSITRON BEAM APPLICATIONS FOR MEASUREMENTS ON WIRE AGING

Positron based measurement techniques are used widely in defect physics due to the high sensitivity to micro defects [15], in particular open volume defects. The lifetime of positrons in a material, or the time positrons exist in a material before annihilating with an electron, is governed by the electron density in the material. In many types of micro defects the atomic density is lower than in the bulk material, resulting in fewer electrons and larger positron lifetime. When entering a material positrons are first slowed down and may migrate for a short time in the material. Since positrons are repelled from atomic nuclei, any region of lower than average atomic density has the effect of attracting positrons and trapping them and this can increase the positron lifetime.

The positron lifetime depends basically on the material and any defects in the material. In a pulsed positron beam both the positron lifetime and the relative intensities of different lifetimes, corresponding to different types of defects, can be measured. Monoenergetic positrons, well defined in time, are directed to a sample and with a fast detector the time to annihilation is measured.

Positrons have proved to be a sensitive probe for both material characterization and defect detection, and have been used for characterization of, for instance, semiconductors, metals and polymers. Within this project positron beam measurements are planned on wires to detect micro defects in the insulation.

For some time a pulsed positron beam has been under construction at Nuclear Engineering, Chalmers University of Technology. During the autumn of 2005 the beam was completed and it is now possible to perform measurements at the facility.

Fig 43. The pulsed positron beam at Nuclear Engineering, Chalmers University of Technology

5.1 The pulsed positron beam

The positrons in the beam are generated by a ^{22}Na continuous positron source. The design of the beam is based mainly on an earlier beam at the University of Ghent, Belgium [16], with some changes. The ^{22}Na radioactive source is contained in a tungsten shielding and in the forward direction the emitted positrons are slowed down and thermalized in a 1 micrometre thick single crystalline tungsten foil.

A schematic overview of the positron beam is shown in figure 44 and the details are further described in [17]. An electric potential of approximately +350 V is applied to both the source and moderating foil to extract the positrons into the beam line. The 350 eV positron beam passes though a chopper, consisting of mainly a copper mesh fed with a sine wave potential, making it possible for the positrons to pass only for a short time every 20 ns. To obtain chopping, the chopper grid is set at an offset potential slightly higher than the source/moderator potential, resulting in a cut-off of the positrons. Adding a sine wave to the offset potential on the grid allows positrons to pass during the negative dip of the applied sine wave. A magnetic guiding system of solenoids with fields of approximately 10 G parallel to the beam line leads the positrons to a 90 degree bend. Here, any unmoderated positrons are separated from the beam while the slow positrons continue through the bend. Compensation for the drift due to the geomagnetic field and external magnetic fields as well as optimization of the field through the bend is achieved by a set of kick coils. After the bend the slow positrons are bunched by a two-gap resonator operating at 50 MHz. After the buncher an acceleration stage accelerates the positrons to a desired voltage, 0-20 kV, in order to facilitate positron penetration into the bulk material and avoid surface effects.

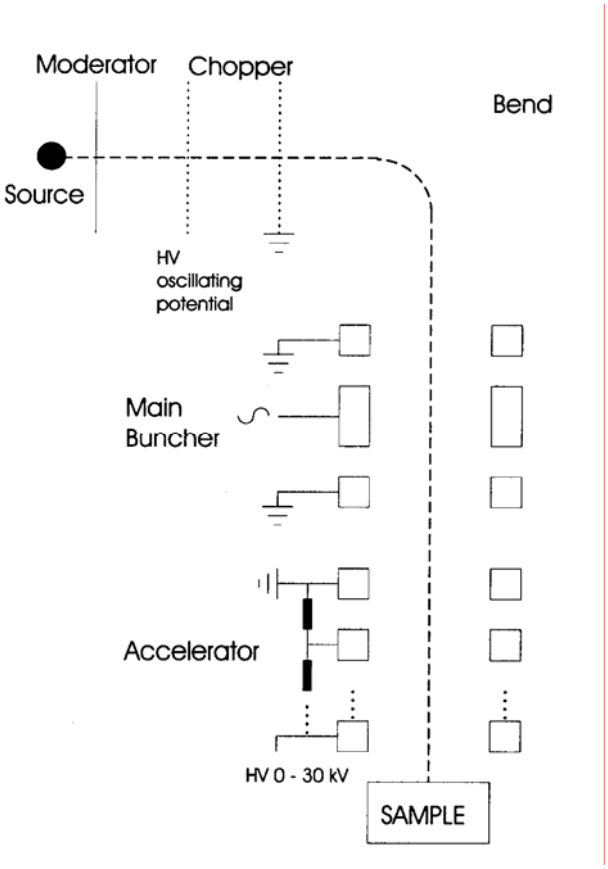

Fig 44. Schematic drawing of the pulsed positron beam

The positron beam then hits the sample, and the annihilation gamma radiation is detected with a fast BaF_2 scintillator beneath the sample holder. The entire beam set-up is contained in a vacuum system.

Both the chopper and buncher use a 50 MHz oscillating signal. For chopping purposes a square wave would be ideal, but at this frequency it is difficult to maintain a square wave form because of capacitive propagation in the beam components. Thus a sine wave is used for both chopping and bunching. The 50 MHz pulsing implies a 20 ns period.

The electronics is shown schematically in figure 45. The 50 MHz is fed via amplifiers both to the chopper, with an offset voltage, and the buncher. The bunching is achieved by the slopes of the sine wave. At the first buncher gap the bunching is performed by the negative slope and at the second gap by the positive slope, with a time of flight between the two gaps corresponding to $\lambda/2$. The system has to be trimmed so that the positron pulse from the chopper arrives at the first gap at the slope of the sine wave. The detector signal is fed through a CF discriminator, with the threshold level adjusted to accept the 511 keV annihilation gamma, and through a delay to the start input of a time-to amplitude converter. The stop signal is generated by a fast gate logic (Universität der Bundeswehr, München), which generates a logical signal at the first positive zero crossing of the 50MHz sine wave after the detector signal. Thus the time directly measured is really the time from the annihilation gamma to next positron pulse.

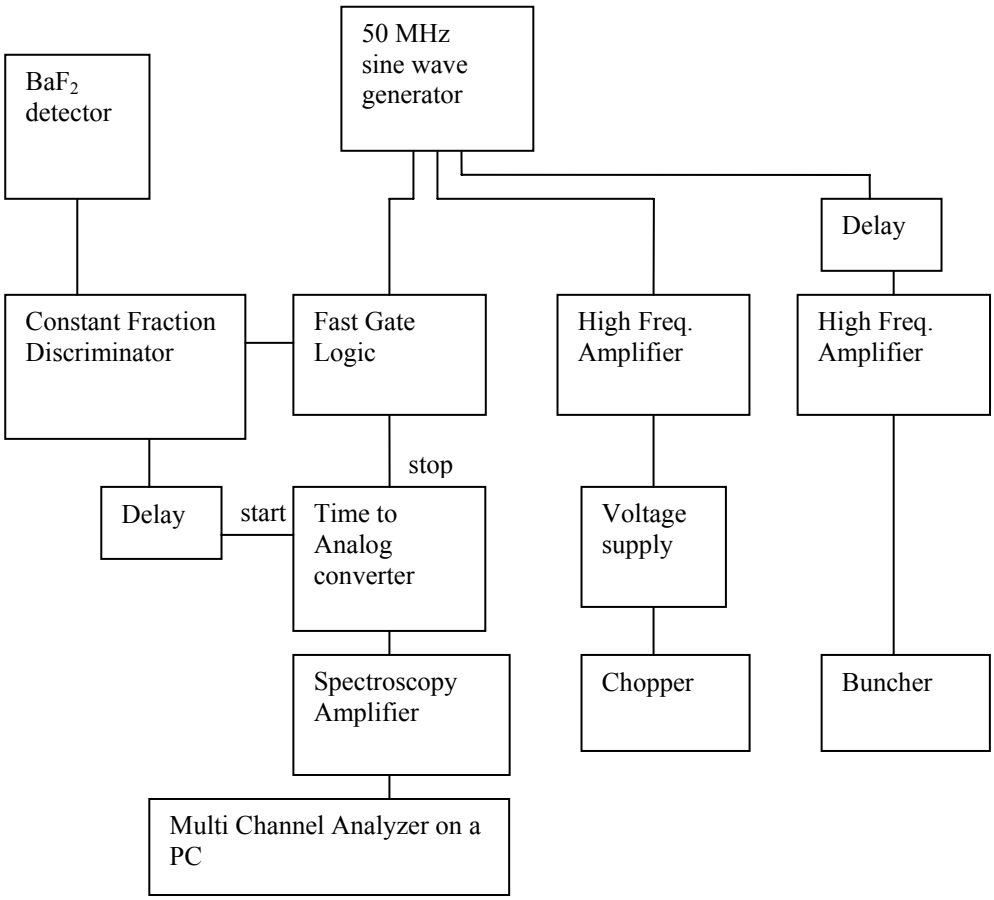

Fig 45. Overview of the electronics

5.2 Data treatment

Much of the technical difficulties in the beam are related to making the positron pulse as well defined in time as possible with a very narrow positron pulse. Even if the pulse width is not directly translated into time resolution of the measurement, the pulse width is of high importance for the time resolution of the measurement, even if it is possible to measure positron half lives well below the width of the positron pulse. In particular the decay time of the pulse in the positron time distribution is of high importance for the time resolution of sample measurements.

The positron decay in a sample can be described as a sum of exponentials. In a simple model with one type of defects, the two exponentials, as shown in figure 46 below, correspond to the defect free material and one type of defects.

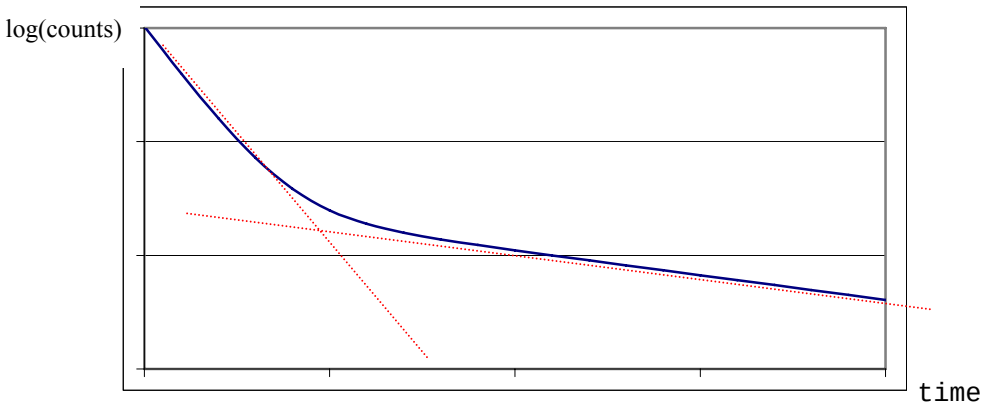

Fig 46. Schematic positron decay time spectrum of bulk material with one type of defect as a sum of two exponential decays

For positrons entering the sample at a fixed time the annihilation gamma time spectrum can be expressed as:

$$\sum_i w_i e^{-\lambda_i t} \tag{58}$$

where i is the number of different lifetime components corresponding to the defect free sample and the different types of defects present in the sample, w_i are weighting factors, λ_i are the different decay constants and t is the time from the positron entering the sample.

Measurements in the ns region and below require special electronics and a fast detector system. The detector is kept relatively small to ensure high time resolution since the time of flight of the photons generated in the scintillator may affect the time resolution for large detectors. Both the detection system and the electronics have a time resolution beneath 50 ps, and the time resolution is determined by the time distributions of the positrons in the pulsed beam. In a pulsed beam measurement the positrons arrive to the sample with the positron time distribution, as shown in figure 47. The width of the peak depends largely on the interplay of the chopper and buncher, while the peak to background ratio mostly depends on the operating conditions of the chopper. It has so far proved that measurements have to be optimized either with respect to the count rate and signal to noise ratio or to the width of the positron pulse, since it has proved very difficult to achieve both. In the measurements on wire measurements will initially be made with pulse width optimization.

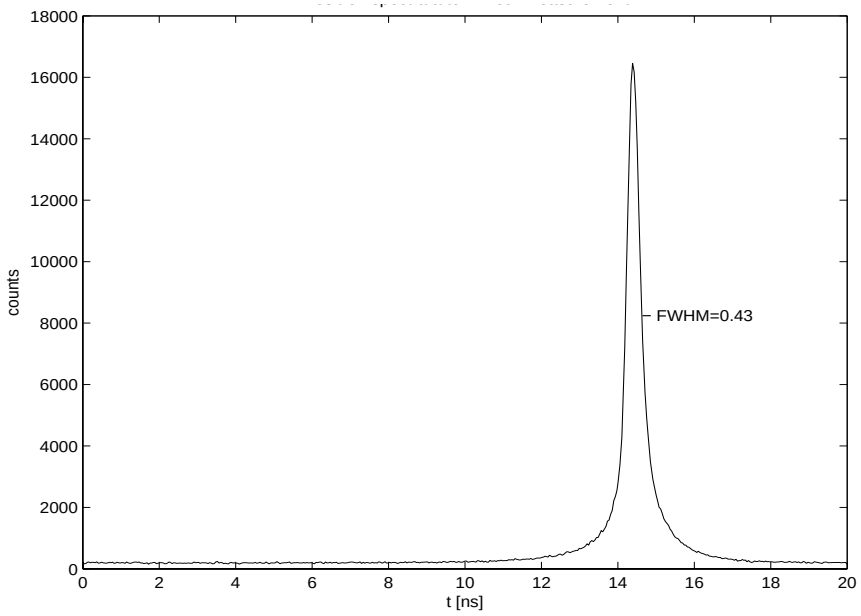

Fig 47. Positron time distribution recorded with multi channel plate detector.

After hitting the sample the positrons decay according to equation (58) above. The resulting measured gamma annihilation time spectrum can then be expressed:

$$spectrum(t) = \sum_{t_{positron}} f(t_{positron}) \sum_{i} w_i e^{-\lambda_i (t + t_{positron})} \tag{59}$$

where $t_{positron}$ is the time when the positrons arrive in the sample with respect to the pulsing system and $f(t_{positron})$ is the positron time distribution, a delta function in an ideal system. An example of a real measurement is shown in figure 48.

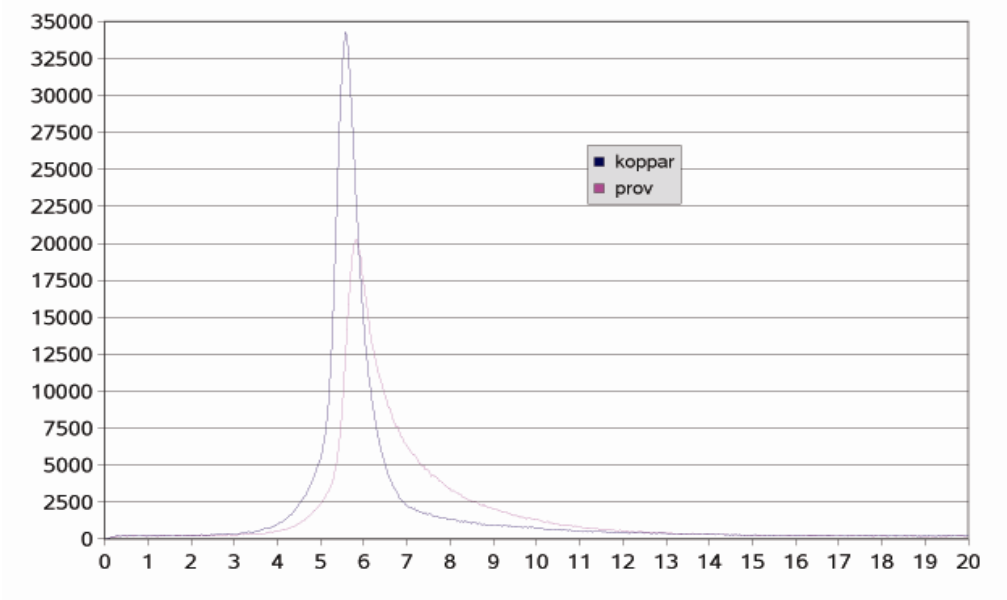

Fig 48. Pulse positron beam measurement with the Chalmers beam on both a copper reference sample (blue, short lifetime) and a semi conductor sample (red, long lifetime). Counts on y-axis and time in ns on x-axis.

From the experimental data we wish to extract decay constants and relative intensities, but these are not directly measured. The methodology when performing a measurement with the beam is first to record the positron time distribution using a sample with very short lifetime (such as well annealed nickel or copper) and to use this time distribution to unfold subsequent measurements. When measuring, both a reference sample without defects to obtain a good characterization of the sample material and samples with defects should be used.

The pilot experiment, shown in fig 48 show both that the positron time resolution in the beam is sufficiently low to perform measurements on samples with larger positron lifetimes and that reasonable statistics can be achieved with a beam time of a few hours. During the spring of 2006 an algorithm for unfolding time spectra from the beam will be developed. This is necessary to handle the large amount of data from the planned measurement series on wires.

5.3 Measurements on wires

Since the samples have to be inserted into the vacuum system of the beam, only relatively small samples can be used, in this respect the measurements technique is destructive since the wire has to be cut. Typical sample size would be around 10x10x5 mm. The samples should be handled in such a way that any defects induced in, for instance, the cutting of the sample does not influence the measurements. The sample chamber is capable of harbouring several samples that can be positioned in the beam without opening the chamber in between. The vacuum system of the beam is also sectioned which makes it possible to open the sample chamber without loss of vacuum in the rest of the beam, although the chamber still has to be pumped after inserting a batch of samples. With this set-up the beam is estimated to handle 2-3 samples per day, depending on the desired time resolution and counting statistics.

Expected lifetimes in cable insulation is in the ns scale, which should easily be resolved with the beam.

Fig 49. The sample chamber with the sample holder (copper) an high voltage and the tube for the scintillation detector below.

The pulsed positron measurement is performed very locally on the wire samples, with a beam diameter of 5 mm. This means that measurements can be performed both on wires at different aging conditions but also, for instance, at different points on a wire that has shown a defect with the LIRA method. Initially measurements are planned on

wire at different aging conditions and this will be carried out in cooperation with KTH and the Ringhals nuclear power reactor.

6. CONCLUSIONS AND FUTURE WORK

The importance of wire systems in industrial installations and in nuclear power plants in particular, is continuing to grow and with that the importance of understanding aging mechanism, aging assessment and condition monitoring techniques to assure that installed wire systems are able to perform their intended function reliably, during all their qualified life. Many results have already been achieved and many research projects are in progress today because a number of issues remain to be resolved, where more efforts and research is needed.

One of the most important unresolved issues is the assessment of condition monitoring techniques for in-situ monitoring of cables, with particular emphasis on I&C safety cables inside the containment. The technique developed at the HRP and described in this report is trying to fill this gap, although more work is still to be done.

The pulsed positron technique at Chalmers University of Technology has been described. Measurements can be performed both on wires at different aging conditions but also, for instance, at different points on a wire that has shown a defect with the LIRA method.

7. ACRONYMS

ANN	Artificial Neural Network
AWG	Arbitrary Wave Generator
BIS	Broadband Impedance Spectroscopy
BNL	Brookhaven National Laboratory
CFR	Code of Federal Regulations
CI	Condition Indicator
CM	Condition Monitoring
COMOR	Comportement des Materiaux Organiques sous Rayonnement
CSNI	Committee on the Safety of Nuclear Installations
CSPE	Chloro-sulfonated Polyethylene
CTG	Cable Task Group
DBA	Design Basis Accident
DBE	Design Basis Event
DOE	U.S. Department of Energy
DSC	Differential Scanning Calorimeter
DUT	Device Under Test
EAB	Elongation At Break
EDF	Electricite' de France
EDT	Excited Dielectric Test
ENB	Ethylene-5 Norbornene-2
EPDM	Ethylene Propylene Dienemonomer
EPR	Ethylene Propylene Rubber
EPRI	Electric Power Research Institute
EVA	Ethylene Vinyl Acetate
FR-	Flame Retardant
FDR	Frequency Domain Reflectometry
FTIR	Fourier Transform Infrared
EQ	Environmental Qualification
FDR	Frequency Domain Reflectometry

I&C	Instrumentation and Control
IAEA	International Atomic Energy Agency
IAGE	Integrity of Components and Structures
IRSN	France Institute for Radiological Protection and Nuclear Safety
IEC	International Electrotechnical Commission
IEEE	Institute of Electrical and Electronics Engineers
IRSN	France Institute for Radiological Protection and Nuclear Safety
JTFDR	Joint Time Frequency Domain Reflectometry
LIRA	Line Resonance Analysis
LOCA	Loss Of Coolant Accident
NASA	National Aeronautics and Space Administration
NEA	Nuclear Energy Agency
NMR	Nuclear Magnetic Resonance
NPP	Nuclear Power Plant
NRC	U.S. Nuclear Regulatory Commission
NRI	Czech Nuclear Research Institute
OIT	Oxidation Induction Time
OITP	Oxidation Induction Temperature
PRBS	Pseudo Random Binary Sequence
PRN	Pseudo Random Number
PSA	Probabilistic Safety Assessment
PVC	Polyvinyl Chloride
PWR	Pressurized Water Reactor
RFS	Resonance Frequency Spread
SKI	Swedish Nuclear Power Inspectorate
SNL	Sandia National Laboratories
TDR	Time Domain Reflectometry
XLPE	Cross-Linked Polyethylene

8. REFERENCES

[1] National Science and Technology Council, Committee on Technology, United States White House, "Review of Federal Programs for Wire System Safety," Wire System Safety Interagency Working Group, November 2000.

[2] IAEA, "Assessment and Management of Ageing of Major NPP Components Important to Safety", IAEA-TECDOC-1188, December 2000

[3] OECD-NEA, "Research Efforts Related to Wire System Aging in Member States", December 2002

[4] Fantoni, F.P., "NPP Wire System Aging Assessment and Condition Monitoring: State-of-the-art Report", HWR-746, March 2004.

[5] Rogovin, D., Lofaro, R.J., Kendig, M., Vora, J., "Application of the Broadband Impedance Diagnostic/Prognostic Technique to Nuclear Power Plant Electric Cables".

[6] "Mesures du facteur de décharges partielle et tangente delta sur câbles HTA type 2000. Evaluation du système de diagnostic BAUR", Rapport d'essais EDF R&D HM-27/02/028/A 2002.

[7] Choe, T.S., Hong, C.Y.,Park J.B., Yoon, T.S., "Implementation of a Time-Frequency Domain Reflectometry System with PXI Platform for a Coaxial Cable", IMTC 2004, Como, Italy, May 18-20, 2004.

[8] Shin, Y.J. et al., "Application of Time-Frequency Domain Reflectometry for Detection and Localization of a Fault on a Coaxial Cable," to appear in *IEEE Transactions on Instrumentation and Measurement*, 2005.

[9] Chang-Liao, K.S., Chung, T.K., Chou, H.P., "Cable Aging Assessment by Electrical Capacitance Measuring Technique", NPIC&HMIT 2000, Washington DC, November 2000.

[10] Waddoups, B., Furse, C., Schmidt, M., "Analysis of Reflectometry for Detection of Chafed Aircraft Wiring Insulation", Fifth Joint NASA/FAA/DoD Conference on Aging Aircraft, Orlando, Florida, Sep. 2001.

[11] Linch, D., "NASA Hybrid Reflectometer Project", Sixth Joint NASA/FAA/DoD Conference on Aging Aircraft, Sep. 2002.

[12] Sinnema,W., "Electronic Transmission Technology", Prentice-Hall, 1988.

[13] Van Putten, A., "Electronic Measurement Systems", Institute of Physics Publishing, 1996.

[14] Allen, R., Mills, D., "Signal Analysis", Wiley Interscience, 2004.

[15] U. Zimmermann, *Positrons in solids*, Paul Scherrer Institute CH-5232 Villigen PSI, 1991.

[16] J. De. Baerdemaeker and C. Dauwe, *Development and application of the Ghent pulsed positron beam*, Applied Surface Science 194, 52-55, 2002.

[17] E. Tengborn and A. Nordlund, *Pilot experiments with the pulsed positron beam at Chalmers University of Technology*, CTH-RF-189, ISSN 0281-9775, Chalmers internal report

Bibliographic Data Sheet **NKS-130**

Title	Wire System Aging Assessment and Condition Monitoring (WASCO)
Author(s)	Paolo F. Fantoni[1] and Anders Nordlund[2]
Affiliation(s)	[1]Institutt for energiteknikk, Norway [2]Chalmers University of Technology, Sweden
ISBN	87-7893-192-4 *Electronic report*
Date	April 2006
Project	NKS_R_2005_43 CableAging
No. of pages	50
No. of tables	2
No. of illustrations	45
No. of references	17
Abstract	Nuclear facilities rely on electrical wire systems to perform a variety of functions for successful operation. Many of these functions directly support the safe operation of the facility; therefore, the continued reliability of wire systems, even as they age, is critical. Condition Monitoring (CM) of installed wire systems is an important part of any aging program, both during the first 40 years of the qualified life and even more in anticipation of the license renewal for a nuclear power plant. This report describes a method for wire system condition monitoring, developed at the Halden Reactor Project, which is based on Frequency Domain Reflectometry. This method resulted in the development of a system called LIRA (LIne Resonance Analysis), which can be used on-line to detect any local or global changes in the cable electrical parameters as a consequence of insulation faults or degradation. LIRA is composed of a signal generator, a signal analyser and a simulator that can be used to simulate several failure/degradation scenarios and assess the accuracy and sensitivity of the LIRA system. Chapter 5 of this report describes an complementary approach based on positron measurement techniques, used widely in defect physics due to the high sensitivity to micro defects, in particular open volume defects. This report describes in details these methodologies, the results of field experiments and the proposed future work.
Key words	Condition monitoring, cable aging, transmission lines, hot spot detection, fault detection, frequency domain reflectometry, time domain reflectometry, standing wave reflectometry, LIRA, positron

Available on request from the NKS Secretariat, P.O.Box 49, DK-4000 Roskilde, Denmark.
Phone (+45) 4677 4045, fax (+45) 4677 4046, e-mail nks@nks.org, www.nks.org